THESIS

CHEMICAL SEPARATIONS OF A FLEROVIUM HOMOLOG USING MACROCYCLIC EXTRACTANTS

Submitted by

Nicole Lynn Ahrens

Department of Environmental and Radiological Health Sciences

In partial fulfillment of the requirements

For the Degree of Master of Science

Colorado State University

Fort Collins, Colorado

Fall 2024

Master's Committee:

Advisor: Ralf Sudowe

Alexander Brandl
Thomas Johnson
Pinar Omur-Ozbek

ABSTRACT

CHEMICAL SEPARATIONS OF A FLEROVIUM HOMOLOG USING MACROCYCLIC EXTRACTANTS

The placement of elements on the Periodic Table is governed by their fundamental chemical properties, maintaining specific trends when they are situated in order of increasing atomic number according to periodic law. When it comes to the heaviest of elements like flerovium (Fl), however, relativistic effects have the potential to alter their chemical behavior relative to lighter elements of the same group. The chemistry of Fl must be studied in order to confirm its placement on the Periodic Table, posing a unique challenge due to its low production cross-sections and short half-life. A chemical system capable of exceptionally fast and selective separations is required to achieve this extreme chemistry task. Such a system can be developed for Fl using its lighter homolog Pb. Two classes of macrocyclic extractants were explored with the aim of developing a chemical separation system for ultimate use in a Fl experiment. Specifically, crown ethers and calixarenes were evaluated as extractants for Pb using extraction chromatography and solvent extraction techniques. In these studies, crown ethers containing both oxygen and sulfur as bridging atoms were found to be ineffective Pb extractants in hydrochloric acid matrices. Unsupported calix[4]arenes also possessing bridging oxygens and sulfurs in various oxidation states were observed to be similarly ineffective but illustrated that the selectivity of calixarenes for Pb can be enhanced by modification of the outer functional groups as well as the bridging atoms. Though not effective as Pb extractants on their own, a significant synergistic effect was observed in EXC studies of a mixed system employing Eichrom Pb resin and a mobile phase containing 4-sulfocalix[4]arene with kinetics suitable for a FI experiment. A similar SX system was then developed using the same crown ether extractant found on Pb resin with carbon tetrachloride as the organic diluent, but Pb extraction by the system was negligible.

ACKNOWLEDGEMENTS

The work presented in this thesis was made possible through the help and guidance of numerous individuals. First, I would like to thank Dr. Ralf Sudowe, my graduate advisor, for his years of support and for granting me the opportunity to pursue this course of study and research. To my technical advisor at LLNL, Dr. John Despotopulos, I'm extremely grateful to you for supporting this research project and for your expert mentorship throughout my time at LLNL. For their instruction and guidance, I am very appreciative of the remaining members of my thesis committee: Dr. Alexander Brandl, Dr. Thomas Johnson and Dr. Pinar Omur-Ozbek. I would also like to thank Dr. Carlos Valdez for his help with synthesizing the macrocyclic extractants that made this research possible. Finally, I wish to thank my incredible family for their unwavering encouragement; and especially my dogs, Ollie and Lulu, for accompanying me throughout this entire journey. Thank you all for your invaluable support.

Lawrence Livermore National Laboratory Disclaimer

This document was prepared as an account of work sponsored by an agency of the United States government. Neither the United States government nor Lawrence Livermore National Security, LLC, nor any of their employees makes any warranty, expressed or implied, or assumes any legal liability or responsibility for the accuracy, completeness, or usefulness of any information, apparatus, product, or process disclosed, or represents that its use would not infringe privately owned rights. Reference herein to any specific commercial product, process, or service by trade name, trademark, manufacturer, or otherwise does not necessarily constitute or imply its endorsement, recommendation, or favoring by the United States government or Lawrence Livermore National Security, LLC. The views and opinions of authors expressed herein do not necessarily state or reflect those of the United States government or Lawrence Livermore National Security, LLC, and shall not be used for advertising or product endorsement purposes.

United States Nuclear Regulatory Commission Funding Auspice Statement

This research was supported under award 5331310021M0028 from the U.S. Nuclear regulatory Commission. The statements, findings, conclusions and recommendations are those of the author(s) and do not necessarily reflect the view of the U.S. Nuclear Regulatory Commission.

TABLE OF CONTENTS

LIST OF TABLES

LIST OF FIGURES

CHAPTER 1: INTRODUCTION

1.1 Background

When a new element is discovered, it is assigned a position on the periodic table based upon its fundamental chemical properties – whether predicted or observed. This ensures the integrity of trends corresponding to atomic size, electron configuration, and chemical behavior. Thus, elements of the same group (vertical column) share homologous chemical properties. However, when a new transactinide element ($Z > 103$) is discovered, it has traditionally been placed in the periodic table solely based on its atomic number, Z, the number of protons in the nucleus. Due to relativistic effects, which increase with Z^2, this placement may not be correct as these superheavy elements may not behave similarly to their direct homologs.[1]

Because of a lack of suitable extraction systems and kinetics, the solution chemistry for some of the very short-lived transactinides has yet to be investigated. However, only through studying the chemical properties of these elements can their correct position on the periodic table be confirmed. As a consequence of the difficulties associated with the production and detection of the heavier transactinides, some of the most basic chemical properties of the superheavies are still unknown. Currently, superheavy element behavior is extrapolated from that of their lighter homologs. Newly discovered heavy elements have been identified first based on their nuclear properties: the nuclear reactions utilized for their formation and their radioactive decay properties.[2] Determination of the chemical properties of the elements is however the most fundamental goal in chemistry.

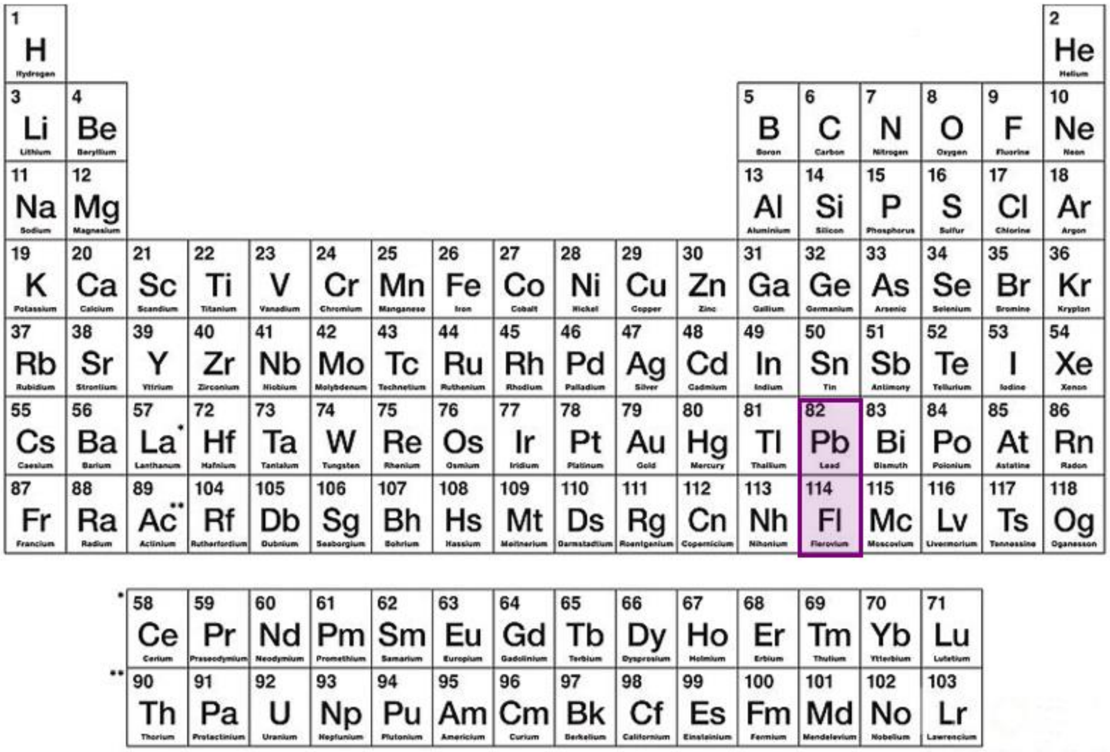

1 H Hydrogen																	2 He Helium
3 Li Lithium	4 Be Beryllium											5 B Boron	6 C Carbon	7 N Nitrogen	8 O Oxygen	9 F Fluorine	10 Ne Neon
11 Na Sodium	12 Mg Magnesium											13 Al Aluminium	14 Si Silicon	15 P Phosphorus	16 S Sulfur	17 Cl Chlorine	18 Ar Argon
19 K Potassium	20 Ca Calcium	21 Sc Scandium	22 Ti Titanium	23 V Vanadium	24 Cr Chromium	25 Mn Manganese	26 Fe Iron	27 Co Cobalt	28 Ni Nickel	29 Cu Copper	30 Zn Zinc	31 Ga Gallium	32 Ge Germanium	33 As Arsenic	34 Se Selenium	35 Br Bromine	36 Kr Krypton
37 Rb Rubidium	38 Sr Strontium	39 Y Yttrium	40 Zr Zirconium	41 Nb Niobium	42 Mo Molybdenum	43 Tc Technetium	44 Ru Ruthenium	45 Rh Rhodium	46 Pd Palladium	47 Ag Silver	48 Cd Cadmium	49 In Indium	50 Sn Tin	51 Sb Antimony	52 Te Tellurium	53 I Iodine	54 Xe Xenon
55 Cs Caesium	56 Ba Barium	57 La* Lanthanum	72 Hf Hafnium	73 Ta Tantalum	74 W Tungsten	75 Re Rhenium	76 Os Osmium	77 Ir Iridium	78 Pt Platinum	79 Au Gold	80 Hg Mercury	81 Tl Thallium	82 Pb Lead	83 Bi Bismuth	84 Po Polonium	85 At Astatine	86 Rn Radon
87 Fr Francium	88 Ra Radium	89 Ac** Actinium	104 Rf Rutherfordium	105 Db Dubnium	106 Sg Seaborgium	107 Bh Bohrium	108 Hs Hassium	109 Mt Meitnerium	110 Ds Darmstadtium	111 Rg Roentgenium	112 Cn Copernicium	113 Nh Nihonium	114 Fl Flerovium	115 Mc Moscovium	116 Lv Livermorium	117 Ts Tennessine	118 Og Oganesson
	*	58 Ce Cerium	59 Pr Praseodymium	60 Nd Neodymium	61 Pm Promethium	62 Sm Samarium	63 Eu Europium	64 Gd Gadolinium	65 Tb Terbium	66 Dy Dysprosium	67 Ho Holmium	68 Er Erbium	69 Tm Thulium	70 Yb Ytterbium	71 Lu Lutetium		
	**	90 Th Thorium	91 Pa Protactinium	92 U Uranium	93 Np Neptunium	94 Pu Plutonium	95 Am Americium	96 Cm Curium	97 Bk Berkelium	98 Cf Californium	99 Es Einsteinium	100 Fm Fermium	101 Md Mendelevium	102 No Nobelium	103 Lr Lawrencium		

Figure 1. Periodic Table of the Elements[3]

1.1.1 The Transactinides

The transactinide (TAN) elements comprise the seventh row of the periodic table beginning at group 4, with the filling of *6d*- orbitals. After the filling of the *6d*- orbitals with elements 104-112, elements 113-118 are expected to complete the seventh row of the periodic table, with the filling of the *7p*- orbitals.[4] When possible, the chemical properties of new heavy elements have been investigated to confirm their properties match the chemical group to which they have been assigned. This is made difficult by several factors. None of the TANs are naturally occurring; instead, they are artificially produced at accelerators a single atom at a time.

Furthermore, the production path of superheavy TANs involves incomplete fusion processes that result in an abundance of by-products that must be removed by physical and/or chemical separation methods. Rapid and very specific separation methods are required due to their relatively short half-lives, followed by specialized detection systems that can reasonably guarantee the observed decay signature came from a single atom of only the target element.[5]

Any chemical system considered must therefore be thoroughly evaluated using the homologs and pseudo-homologs of the desired TAN before it can be used in a TAN chemistry experiment. The typical production rate of superheavy elements such as $^{287\text{-}289}$Fl is anywhere between 0.5 and 5 atoms per day, depending on experimental parameters including target material and thickness. Consequently, their investigation is limited to the scale of atom-at-a-time chemistry.[6] In principle, the statistical validity of experimental results of two-phase systems for superheavy elements produced atom-at-a-time can be upheld by an equilibration formulation derived from a law of mass action in which the probabilities of finding an atom in a given phase are used in place of concentrations.[5] Additionally, the kinetics of the chemical system must be comparable to the half-life of the radionuclide being investigated. The selectivity of the chemical system for a specific element is very important for the superheavies due to their low cross-sections, which range from picobarns to femtobarns for the production of elements with $Z > 108$.[7,8,9,10,11,12,13] The decay characteristics of each Fl isotope studied must be known well enough and be suitably unique for positive identification when it comes to detection of one atom at a time. This is an especially difficult feat in the case of isotopes undergoing spontaneous fission (SF), e.g., ^{284,286}Fl.[14]

Aqueous studies of the TANs with $Z < 106$ have been completed in the past with a variety of methods: the earliest utilized manual or automated liquid-liquid extraction and ion exchange, which consisted of a sample collection time, followed by sample dissolution, chemistry, and finally decay counting. These experiments could be performed in approximately 50 s with cycles occurring every 60 to 90 s.[15] This was possible due to the longer half-lives of these early TAN, e.g., ^{261}Rf ($t_{1/2} = 65$ s), and the higher production rates of these elements (atoms/minute). With the heavier TANs, production rates – and the resulting detection rates – fall significantly (a few atoms per day or even atoms per week), necessitating the development of fast (^{289}Fl $t_{1/2} = 2.1$ s), automated chemical systems. The combination of advanced relativistic quantum chemical calculations with experimental data is necessary to understand TAN chemistry. Physical separation of interfering reaction products has been achieved for gas-phase studies via gas-filled pre-separators such as the TransActinide Separator and Chemistry Apparatus (TASCA) or the Berkeley Gas-Filled Separator (BGS), but aqueous chemical separation has yet to be achieved for Fl isotopes due to a number of limitations including production rates, cross sections, decay modes and short half-lives.[6]

1.1.2 Relativistic Effects

Relativistic effects arise when the inner electrons attain relativistic speeds, with an associated relativistic mass increase, and these effects increase with Z^2. The relativistic mass increase causes a spatial contraction of the inner electron orbitals, increasing the binding energy and the electronic shielding of the nuclear charge seen by outer electrons. Due to this modified electronic shielding, and because of the orthogonality of all electronic orbitals, these relativistic effects propagate to the outermost (non-relativistic) electron orbitals. The resulting effect on the valence electrons, which largely determine the chemical properties, is a decrease in radius and an increase in binding energy for orbitals with low-angular momentum, *l*, and an increase in radius and decrease in binding energy for high-*l* orbitals.[16] Another effect of interest in the heaviest elements, often included in descriptions of relativistic effects, is spin-orbit splitting for orbitals with $l > 0$. Spin-orbit splitting changes the energy of electron orbitals, depending on the alignment of the intrinsic electron spin with the electron orbital angular momentum. The effect increases with Z^4, lowering the energies of l-1/2 orbitals and raising the energies of l+1/2 orbitals.[17] In the valence electrons of the TAN elements, the magnitude of spin-orbit splitting is comparable to that of the other relativistic effects.

Due to the high nuclear charge of TANs, electrons are accelerated to relativistic speeds, contracting the innermost orbitals and increasing shielding in the outer orbitals, which in turn affects electron mass, energy levels and chemical bonding characteristics.[2,4] These relativistic effects change the relative energies of electronic orbitals, changing the electron filling order and potentially disrupting the periodic table structure as derived from the chemical properties of lighter, less-relativistic elements. The changes in orbital energies and radial extents will have a strong effect on chemical bonding, bringing about changes in the chemical properties of superheavy elements.[17] Such changes have been reported for Rf, Db, Sg, and Cn.[16,19,20] Fl is especially important to study, as it is located on the periodic table in the area where relativistic effects are expected to significantly change its chemical properties with respect to its lighter homologs.[2]

1.2 Flerovium

Element 114 was discovered via the ^{244}Pu(^{48}Ca,3n)^{289}114 reaction at the U400 heavy ion cyclotron in Dubna, Russia, in 1998 through a collaboration between the Joint Institute for Nuclear Research (JINR) and Lawrence Livermore National Laboratory (LLNL) (*fig.2*).[7] Joint efforts by JINR, LLNL and Lawrence Berkeley National Laboratory (LBNL) led to the discovery of five additional isotopes of element 114 over the next fifteen years.[8,9,10,11,12,13] Element 114 was officially placed on the Periodic Table under the name flerovium in 2012.[3] Table 1 shows currently acknowledged decay data for the six known isotopes of Fl: four of the six known isotopes of Fl undergo α-decay within a few seconds, while the decay modes of ^{286}Fl are practically split between α-decay and spontaneous fission and ^{284}Fl decays via spontaneous fission with a half-life on the order of milliseconds.[7,8,9,10,11,12,13,21,22,23]

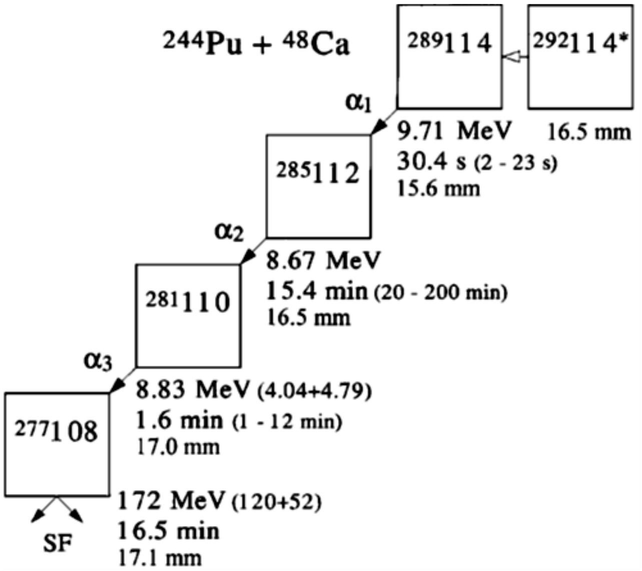

Figure 2. Observed decay chain upon initial discovery of element 114[7]

Table 1. Published decay properties of $^{284\text{-}289}$Fl

Nuclide	Decay Mode	Half-life	E_α (MeV)	Ref.
^{289}Fl	α	2.1 ± 0.6 s	9.95 ± 0.06	[7,21]
^{288}Fl	α	0.65 ± 0.1 s	9.94 ± 0.08	[9, 10,11,21]
^{287}Fl	α	0.36 ± 0.2 s	10.01 ± 0.07	[8,10,11,21,22]
^{286}Fl	α≈60%; SF≈40%	130 ± 30 ms	10.19 ± 0.06	[10,11,21,22]
^{285}Fl	α	0.15 ± 0.8 s	10.41 ± 0.05	[12,13,23,21]
^{284}Fl	SF	2.5 ± 1.3 ms		[13,23,21]

1.2.1 Predicted Properties of Fl

Fl is the first element theoretically predicted to show large deviations from expected periodic trends, as seen in the conflicting theories that exist for element 114 – some indicate a noble, gaseous state while others foresee an extraordinarily volatile metal.[24] One persistent prediction based on atomic calculations indicated that elements 112, 114, and 118 may be gaseous, and even as inert as a noble gas.[25] More recently, numerous first-principles calculations have been made for Fl using the pseudopotential method and density-functional theory (DFT). The electronic and ground state properties of Fl have been investigated using the pseudopotential method; it is predicted to adopt a hexagonal-close-packed structure.[26] Studies using DFT suggest that Fl is metallic.[27] By decomposing the total energy into many-body forces derived from relativistic coupled-cluster theory and DFT, the melting point of Fl was predicted to be below room temperature.[28] Modern, fully relativistic calculations suggest that Fl is a volatile metal and will be adsorbed on a Au surface through metal-metal bond formation.[29]

1.2.2 Flerovium Experiments

Gas-adsorption chromatography experiments have largely prevailed across the entire range of superheavy elements. The first gas-phase experiment for element 114 was performed at the Flerov Laboratory for Nuclear Reactions (FLNR) in Dubna, in which three Fl atoms were deposited on a Au-surface detector at varying temperatures, which concluded that this was due to physisorption.[30] This was contradicted when an experiment at the Gesellschaft für Schwerionenforschung (GSI) in Darmstadt, Germany, using the same chemical techniques coupled to a gas-filled pre-separator (TASCA, *fig.3*) at room temperature, indicated that Fl adsorbs to a Au surface through the formation of metal-metal bonds.[31] Fully relativistic calculations are in agreement with the latter experimental findings, and recently received further support with the observation of six additional Fl atoms by the GSI group.[29,32] The current consensus is that Fl is the most volatile metal in the periodic table and the least reactive member of group 14, though not as inert as Rn, and likely a liquid at room temperature.[28,32]

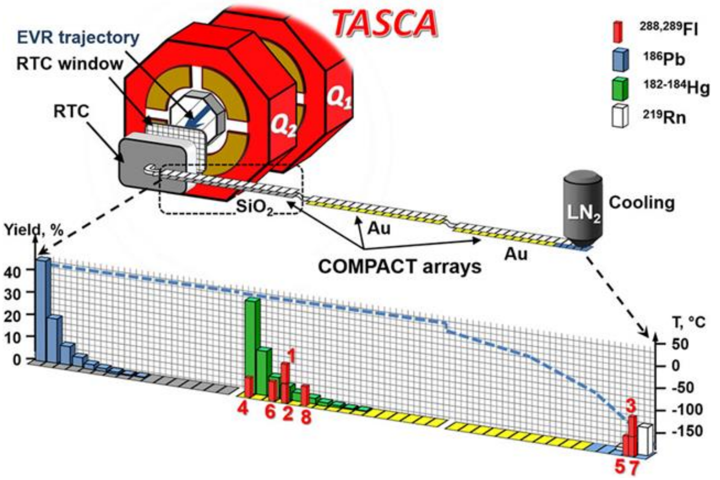

Figure 3. The gas-filled TransActinide Separator and Chemistry Apparatus (TASCA) [32]

1.1 Homolog Chemistry

Homolog and pseudo-homolog studies are also used to develop and test chemical systems for their ultimate use in TAN experiments. A “homolog” here refers to an element in the same group on the Periodic Table and having similar chemical properties. From extrapolation of periodic trends, elements belonging to different groups but having the potential to behave similarly are considered pseudo-homologs. Because the short half-lives of Fl isotopes preclude their chemical systems from ever reaching a true equilibrium state, the chemical properties of their atoms at a pseudo-equilibrium state can be extrapolated from the behavior of their homolog elements.[6] These studies can either be conducted in two ways: by performing rapid chemical separations during on-line production of the homologs at an accelerator, or off-line using carrier-free, ultra-trace radionuclides. Lead is a homolog of flerovium, situated directly above it in Group 14 of the Periodic Table.[3]

CHAPTER 2: CHEMICAL SEPARATIONS

2.1 Extraction Chromatography

Extraction chromatography (EXC) is a prominent chemical separation technique which combines the efficiency and selectivity of solvent extraction with the multistage character of chromatographic methods. This simple technique is well-suited to the rapid separation and preconcentration of radionuclides in trace amounts from a wide range of sample matrices.[33] An EXC system is comprised of three major components: an inert support, a stationary phase, and a mobile phase.

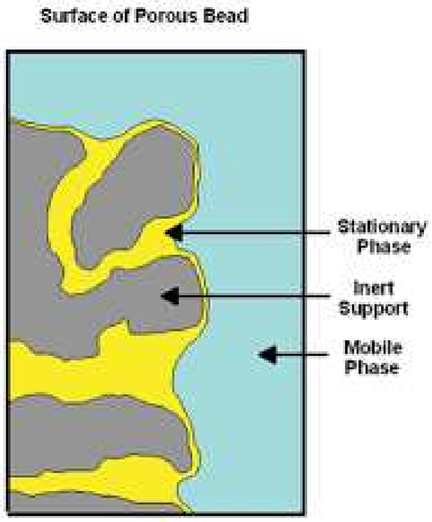

Figure 4. Cross section view of an EXC column showing the stationary phase coating the resin[34]

The solid support usually consists of chemically inert beads made of porous silica or an organic polymer ranging from 50 to 150 µm in diameter. A chemically inert material is required in order for the support not to interfere with the reactions taking place between the mobile and stationary phases.[33,35] The stationary phase is composed of a liquid extractant immobilized in the pores of the solid support. Extraction chromatographic resins are typically prepared by coating the beads with a solution of the extractant in a volatile solvent and then slowly evaporating off the solvent, leaving the extractant physically bound to the inert support and lending complex forming abilities to the stationary phase.[33,36] The mobile phase is an aqueous solution that comes into contact with the resin and competes with the stationary phase for the radionuclide of interest. Changes to both the stationary and mobile phases can be tailored to alter the retention of a particular analyte by a resin, making it possible to finely tune an EXC system for a specific purpose.[37]

EXC is a form of solvent extraction in which the stationary and mobile phases are the organic and aqueous phases, respectively. More effective resins can be developed by optimizing the composition of their stationary phase with novel organic extractants and suitable diluents. The choice of organic diluent can affect both the efficiency and selectivity of metal complex extractions, in particular. As in solvent extraction, the adsorption of a metal ion by EXC also involves the conversion of a hydrated metal ion into an uncharged, organophilic complex.[36,38] Due to their close relationship, solvent extraction experiments are a common preliminary method used to identify organic extractants and diluents in the design of new EXC systems, and vice versa.

2.1.1 Weight Distribution Ratios and Column Capacity Factors

For EXC systems, the distribution ratio (D) and column capacity factor (k’) are not measured directly, but calculated from the weight distribution ratio, D_w. This is due to the fact that the stationary phase is bound to the resin and therefore in a different physical state than the aqueous mobile phase.[37] The weight distribution ratio, D_w, is calculated by measuring the activity of the analyte of interest adsorbed by a known mass of resin from a given volume of aqueous solution using the equation:

$$D_w = \frac{A_r}{A_s} = \frac{A_0 - A_s}{A_s} \times \frac{mL}{g} \qquad \text{(Eqn. 1)}$$

where A_0 is the initial activity, A_r is the activity sorbed on a known amount of resin, g, and A_s is the activity in a known volume, mL, of solution. The D_w can then be converted directly to the number of free column volumes to peak maximum, k’, using a resin factor, F_c, provided by the manufacturer:

$$k' = \frac{D_w}{F_c} \qquad \text{(Eqn. 2)}$$

2.2 Solvent Extraction

Solvent extraction (SX), or liquid-liquid extraction, is another common technique used in radiochemistry to separate compounds based on their solubility in different solvents. The principles of solvent extraction involve several fundamental concepts including partitioning, selectivity, concentration, polarity, temperature, and time. Partitioning refers to the distribution of a solute between two immiscible solvents based on the solubility of the solute in each solvent (phase). Selectivity in SX refers to the ability of a solvent to preferentially select the solute of interest while excluding others. Different solvents have varying affinities for different solutes, which allows for highly selective extraction in finely tuned systems. Generally, an organic and an aqueous solvent are used in which the solute has a different solubility in each phase and a separation is achieved once the solute has distributed itself into one of the phases.[39] Therefore, the distribution ratio of a SX system is represented by:

$$\mathrm{D} = \frac{[\mathrm{A}]_{\mathrm{org}}}{[\mathrm{A}]_{\mathrm{aq}}} = \frac{\mathrm{V}_{\mathrm{aq}} \times \mathrm{A}_{\mathrm{org}}}{\mathrm{V}_{\mathrm{org}} \times \mathrm{A}_{\mathrm{aq}}} \qquad \text{(Eqn. 3)}$$

where $[\mathrm{A}]_{\mathrm{org}}$ is the concentration of solute in the organic phase and $[\mathrm{A}]_{\mathrm{aq}}$ is the concentration of solute in the aqueous phase, and V_{aq} and $\mathrm{V}_{\mathrm{org}}$ are the volumes of the aqueous phase and organic phase, respectively. In the systems described herein, the volumes are the same and the equation for the distribution ratio can be simplified to:

$$\mathrm{D} = \frac{(\mathrm{A}_0 - \mathrm{A}_{\mathrm{aq}})}{\mathrm{A}_{\mathrm{aq}}} \qquad \text{(Eqn. 4)}$$

where A_0 is the initial activity of the solute, A_{aq} is the activity of the solute in the aqueous phase, and $(\mathrm{A}_0 – \mathrm{A}_{\mathrm{aq}})$ equals the activity of the solute, $\mathrm{A}_{\mathrm{org}}$, in the organic phase. After sufficient mixing time has passed such that the net change of the concentration of solute amongst the phases remains constant, the distribution ratio is calculated to quantify how the solute divides itself between the two phases.[40] The distribution ratio, D, can be converted to the extraction fraction (percentage extracted) by:

$$\%\mathrm{E} = \frac{100 \times (\mathrm{A}_0 - \mathrm{A}_{\mathrm{aq}})}{\mathrm{A}_0} = \frac{100\mathrm{D}}{(1+\mathrm{D})} \qquad \text{(Eqn. 5)}$$

where a distribution ratio of 1 equates to 50% extraction, indicating an even distribution of the solute between phases, and a distribution ratio of 100 indicates >99% extraction.[39]

This process can be influenced by the initial concentration of the solute, with higher concentrations often leading to greater efficiency in the extraction.[39] For ultra-trace level chemistry, therefore, a SX extraction system with a very large distribution ratio is required to achieve efficient, highly selective extractions.[6] Polarity is also an important consideration since the two liquid phases need to be immiscible, and non-polar solvents are used to extract non-polar substances and vice versa. Temperature can influence solubility and, consequently, the efficiency of the extraction process.[39] Extraction in a SX system takes place at the phase boundary and the time it takes for the system to reach equilibrium can be decreased by increasing the surface area of the phase boundary via vigorous mixing. Mixing causes each solvent to finely disburse in the other.[39,40] After mixing, the immiscible liquid phases will spontaneously separate into two distinct layers based on their densities. The resulting separation occurs due to the different solubility of the solute in the two solvents.

In order to achieve a sufficient separation of a solute at the ultra-trace scale, the distribution ratio for a given SX system must be maximized as much as possible.[6] Chemical modification, such as addition of an extractant molecule that forms complexes with the solute (e.g., macrocycles) to the organic solvent, can enhance selectivity and increase the distribution ratio.[39] This is a major advantage of SX, as it enables the tuning of a system to be highly selective for an individual analyte of interest. The efficiency of SX is another advantage that can be exploited for studies utilizing very short-lived radionuclides. It is for these reasons that SX will be a primary technique employed in this research.

2.3 Macrocyclic Extractants

Atom-at-a-time chemistry will require specialized chemical separation systems that are both extremely fast and tremendously selective for elements of interest. As applies to coordination chemistry, “macrocycles” are cyclic macromolecules having three or more donor atoms for coordination to metal centers.[4] Two particular classes of macrocyclic ligands have shown promise in Fl and Cn homolog studies: crown ethers and calixarenes. [44,51] Crown ethers show the required level of extraction specificity but are considered to be kinetically slow, whereas calixarenes perform rapid separations but display selectivity for more than one periodic group. The study of TANs will require unique, specialized molecules based upon one or both of these specialized macrocycles.

2.3.1 Crown Ethers

Crown ethers are macrocyclic polyethers capable of forming host-guest complexes. Extraction by crown ethers occurs based on electrostatic ion-dipole interactions between the negatively charged ring atoms (oxygen, sulfur, etc.) and positively charged metal cations. Crown ethers show a high selectivity for metal cations of comparable diameter to that of the negatively charged crown cavity and tend to form very stable 1:1 metal-crown complexes.[52] The increased binding stability of metal cations by a cyclic polyether compared to that of an open ring is called the macrocyclic effect, which gives rise to this notable complex stability.[53] The crown ether 18-

crown-6 (cavity diameter 2.6 – 3.2 Å) (*fig.5*) is known to form positively charged complexes via coordination with a hydronium ion (H_3O^+), which in turn can be utilized to extract positively-charged metal complexes. [54,55]

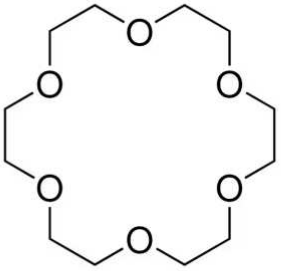

Figure 5. The crown ether 18-crown-6

Thiacrown ethers, in which the substitution of oxygen with sulfur results in an even greater specificity for soft metals, have previously been synthesized at LLNL and studied with Fl homologs. The sulfur analog of DtBuCH18C6, DBHT18C6, displayed vastly improved kinetics for Hg.[44,45,46] The investigation of crown ethers as extractants at LLNL was continued in this work by looking at aqueous complexants to aid Pb extraction (e.g., calixarenes).

2.3.2 Calixarenes

Calixarenes are macrocyclic oligomers comprised of phenolic units meta linked by methylene bridges, taking the shape of a conical vase or chalice (in Greek, “calix”).[56] A number, n, representing the number of repeating phenolic units is inserted between the “x” and “a” in “X-xCalix[n]arene” to designate the size of the macrocyclic ring (*fig.6*). The prefix “X” refers to the upper rim functional groups. Their inner cavities, which are available to host-guest type interactions with the solutes, are able to accommodate various guest molecules similarly to crown ethers.[56,57] Therefore, calixarenes can also be used to manipulate selectivity. This selectivity is due to the presence of the cavity as well as to the outer functional groups.[44,57,58] Solvent extraction studies have demonstrated that the coordination ability of the calix[4]arenes depends on the bridging x, as seen in Figure 6.[51,58] While calixarenes can be used to change selectivity in several separation techniques, this work will explore their use in extraction chromatography and solvent extraction only.

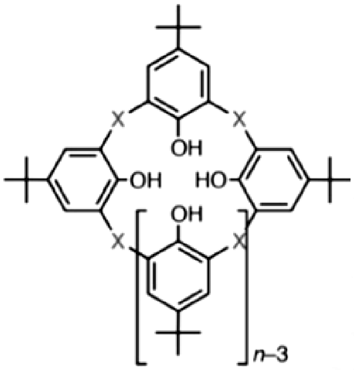

	X	*n*
C*n*A	CH_2	4
TC*n*A	S	4
SOCA	SO	4
SO_2CA	SO_2	4

Figure 6. Molecular structure of calix[4]arenes with various sulfur-based bridge constituents

2.4 Review of Previous Studies in Literature

As previously discussed, theoretical predictions and gas-phase studies comprise a significant majority of the work that has been performed to elucidate the chemical behavior of Fl. The first experiments with Fl homologs and pseudo-homologs intended specifically for the development of an aqueous chemical system for Fl consisted of generator studies, which determined that Pb could be continually eluted from a solution of ^{223,228}Ra, ^{227,228}Th, or ^{227,228}Ac sorbed onto a Dowex 50x8 column.[41,42] This method was later refined to produce a generator using ^{228}Th loaded onto an AG 50Wx8 cation exchange column from which ^{212}Pb can be eluted from an HCl matrix.[43] This second generator was then used in Fl homolog studies with sulfur macrocyclic extractants (*fig.7*), which showed no selectivity for Pb(II).[44,45,46]

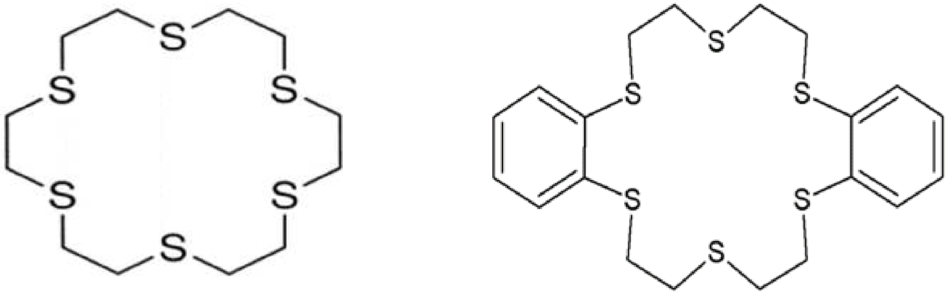

Figure 7. Hexathia-18-crown-6 (HT18C6) and Dibenzo-hexathia-18-crown-6 (DBHT18C6)

To date, two sulfur macrocyclic extractants have been studied by *Despotopulos et al.* for the development of a TAN chemical system using homologs and pseudo-homologs of elements 112 and 114: hexathia-18-crown-6 ether (HT18C6) and dibenzo-hexathia-18-crown-6 (DBHT18C6), shown above in Figure 7.[44,45,46] These studies were based on the ability of the crown ether extractant di-*tert*-butylcyclohexano-18-crown-6 (DtBuCH18C6) to extract lead (Pb) and mercury (Hg), but with kinetics too slow for TAN experiments;[44] and the high selectivity and fast kinetics of Hg extractions using a thiacrown ether.[47,48] The substitution of oxygen in the ring with sulfur was expected to make the 18-crown-6 base structure more specific for soft metal (such as Hg and Pb) chemistry, theoretically solving the kinetics problem. In solvent extraction studies, HT18C6 was found to extract Hg faster than DtBuCH18C6 but it did not extract Pb at all (*fig.8*). The extremely low solubility of HT18C6 in the organic solvent also precluded attempts to elucidate the speciation of the extracted complex.[45,46]

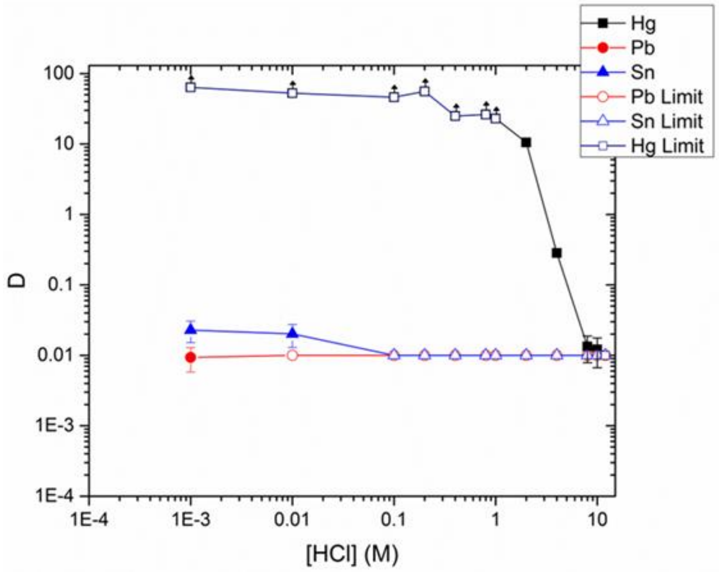

Figure 8. The extraction of Pb homologs and pseudo-homologs by HT18C6[46]

A second thiacrown ether, DBHT18C6, was then synthesized by the same group in an attempt to elucidate the effects of crown conformation on metal complexation.[45] Traditional crown ethers possess a cavity as a result of their endodentate conformation, orienting a pocket of charge density towards the center of the ring. Thiacrown ethers, on the other hand, tend to have their sulfurs oriented in an exodentate manner. This means that thiacrown ethers may have unique extraction mechanisms and distortion into an endodentate conformation will be necessary for them to coordinate with a metal cation similarly to the traditional crown ether.[49,50] DBHT18C6, having a negative charge region analogous to the traditional crown ether, was expected to extract Pb analogous to DtBuCH18C6; however, DBHT18C6 also did not extract Pb (*fig.9*). [45]

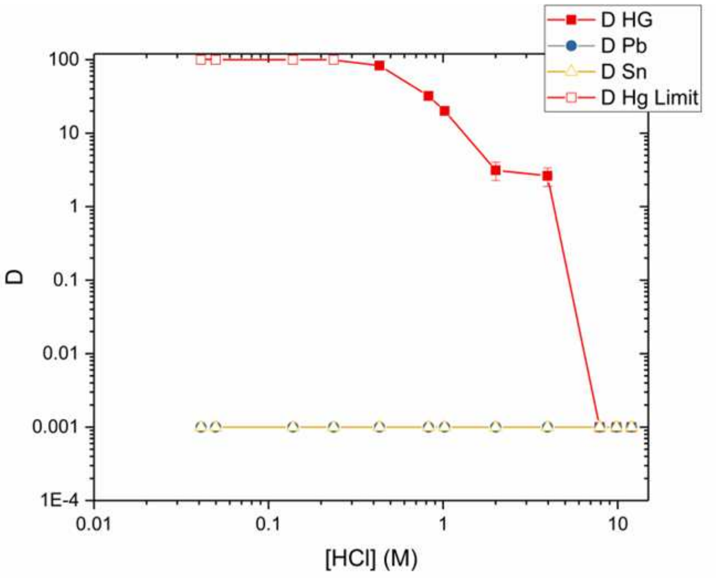

Figure 9. The extraction of Pb homologs and pseudo-homologs by DBHT18C6 [45]

2.5 Research Objective

The focus of this research is to find a suitable extractant that exhibits both a strong affinity and fast kinetics for lead. The macrocyclic ligands discussed above can also be utilized to predict other chemical behaviors of TANs. Homolog studies can be performed to deduce size (from cavity size), speciation (based on elution versus counter ion), and complexation (based on halide complexation).[15] For example, by changing the counter ions in the system, we can change the complexation and deduce speciation based on the behavior of homolog elements. Anionic complexes can also be tuned using halide counter ions, wherein the cation goes into the cavity and the ion of interest forms an anion that complexes strongly with halides. Experiments with a short-lived isotope of Pb, a group 14 homolog of Fl, was carried out.[43] The efficiency and selectivity of the separation systems was evaluated for potential use in a Fl experiment to ultimately assess the impact of relativistic effects on the chemical properties of the superheavy TAN elements.

CHAPTER 3: ANALYTIC TECHNIQUES

Any chemical system must be thoroughly evaluated using the homologs and pseudo-homologs of the desired TAN before it can be used in a TAN chemistry experiment. Extraction chromatography (EXC), solvent extraction (SX), and high purity germanium gamma spectroscopy techniques were used in the investigation of lead-212 as a Fl homolog. The general procedure for each technique is presented below, along with an overview and explanation of the data analyses used herein. Materials and reagents are listed in Appendix I.

3.1 Lead-212 generator

All radiolead used in this work was obtained from a generator developed for the continuous elution of ^{212}Pb from the parent radionuclide ^{228}Th by *Despotopulos et al*.[43] The generator was prepared by loading approximately 100 µCi of ^{228}Th (derived from ^{232}U legacy material) in 1 mL of 0.4 M HCl onto a preconditioned 2.5 mL AG 50Wx8 (100-200 mesh) cation exchange column. The column was rinsed with 10 mL of 0.4M HCl and stored for 3 days to allow for > 99% ingrowth of ^{212}Pb (72 h, approximately 7 half-lives of ^{212}Pb, yields 99.1% equilibrium with parent). At the beginning of each study, ^{212}Pb was eluted from the column with 2 mL of 2 M HCl and added directly to samples, and the column was re-conditioned with 2 mL 0.4M HCl before being stored for subsequent experiments. The decay chain of ^{228}Th is shown in Figure 10.

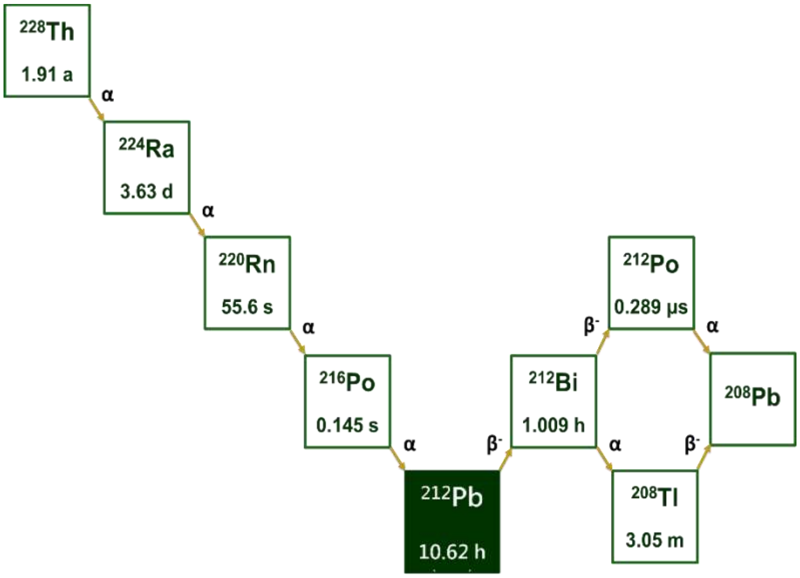

Figure 10. Thorium-228 decay chain with half-lives[21]

Generators such as this allow for the continuous, long-term procurement of carrier-free radionuclides. The term "carrier-free" indicates 100% isotopic abundance. The spectral line with the highest relative yield was chosen for determining the activity of ^{212}Pb in all samples by HPGe gamma-ray spectroscopy (Table 2).

Table 2. Photon energies selected for activity determination[59]

Radionuclide (half-life)	Energy (intensity, %)
^{212}Pb ($t_{1/2}$ = 10.62 h)	238.6 keV (43.3%)

3.2 Extraction Chromatographic Resin

EXC batch studies were performed with the commercially-available Pb resin obtained from Eichrom Technologies, which contains the crown ether 4',4"(5")-di-*tert*-butyldicyclohexano-18-crown-6 (DtBuCH18C6) (*fig.11*) and has been well-characterized for its lead uptake (*fig.12*).[60,61] In a previous study by *Horwitz et al.*, Pb resin exhibited a very high extraction of lead in nitric acid media ($k'_{max} \approx 800$) and moderate Pb extraction in hydrochloric acid media ($k'_{max} \approx 150$).[60] The conversion factor F_C for Pb resin is 1.82.[60] EXC resins can be characterized by measuring parameters such as D_w and k' in batch uptake experiments, in which free resin is used instead of a column.

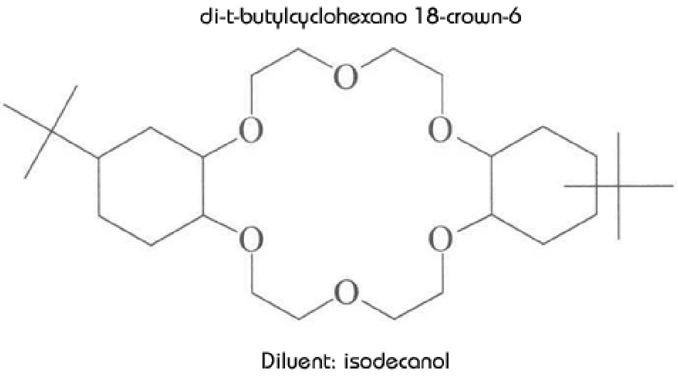

Figure 11. Molecular structure of the crown ether extractant used in Pb resin[61]

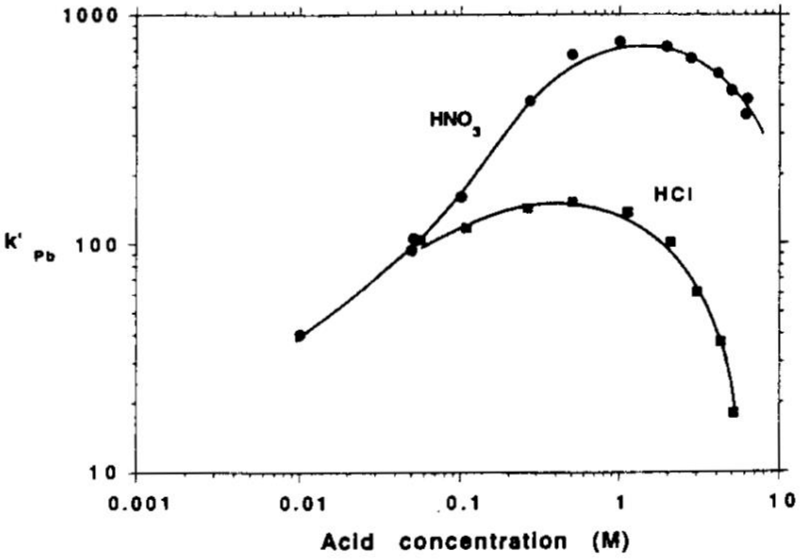

Figure 12. Nitric and hydrochloric acid dependencies of k’ for lead on Pb resin[60]

3.3 Crown Ether

The commercially available crown ether 4’,4”(5”)-di-tert-butyldicyclohexano-18-crown-6 (DtBuCH18C6) (*fig.11*) was used as an extractant in carbon tetrachloride (CCl_4) as the organic phase for SX studies with the Fl homolog ^{212}Pb. DtBuCH18C6 (484.71 g mol^{-1}) was purchased from Sigma-Aldrich and melted on a hot plate for ease of handling prior to dilutions with CCl_4. The liquified crown ether was pipetted into volumetric flasks on a balance then brought to volume with CCl_4 following the scheme in Table 3.

Table 3. Stock solutions prepared for SX studies with 4’,4”(5”)-di-*tert*-butyldicyclohexano-18-crown-6

[DtBuCH18C6] (M)	Mass DtBuCH18C6 (g)	Volume (mL)
0.001	0.0024	5
0.005	0.0121	5
0.01	0.0969	20
0.05	0.1211	5
0.06	0.3000	10
0.1	0.2423	5

3.4 Calixarenes

4-*tert*-butylcalix[4]arene (C4A), 4-*tert*-butylthiacalix[4]arene (TC4A) and 4-*tert*-butylsulfonylcalix[4]arene (SO_2CA) were used as extractants dissolved in chloroform ($CHCl_3$) as the organic phase for SX studies (*fig.13*). The calixarenes were obtained in solid form from commercial vendors and were massed out for dilution with $CHCl_3$ according to the scheme in Table 4.

Table 4. Stock solutions prepared for SX studies with calixarenes in $CHCl_3$

Calixarene	[Calixarene] (M)	Calixarene Mass (g)	Volume (mL)	Calixarene MW (g/mol)
C4A	0.001	0.0130	20	648.91
TC4A	0.001	0.0144	20	721.06
SO_2CA	0.001	0.0170	20	849.05

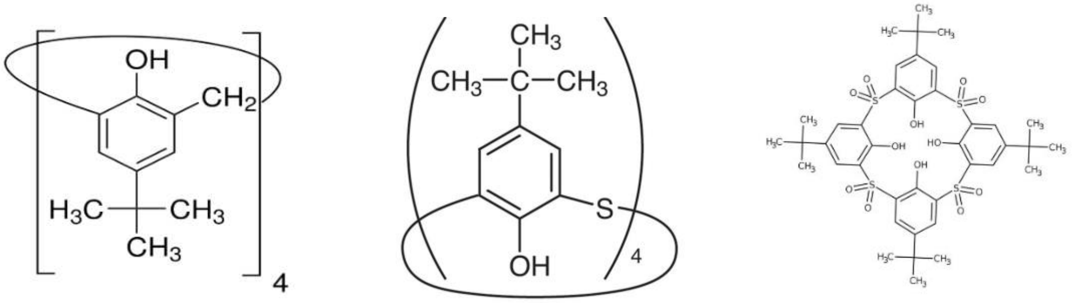

Figure 13. Molecular structure of the calix[4]arenes C4A (left), TC4A (middle), and SO2CA (right)

4-sulfocalix[4]arene (SC4A) was the only water-soluble calixarene investigated and was added to the mobile phase for batch studies with Eichrom's Pb resin and to the aqueous phase for SX studies with DtBuCH18C6. SC4A (*fig.14*) has a molecular weight of 744.74 g mol^{-1}, which was used to calculate the mass required to make 1 mM solutions of sulfocalix[4]arene in the various nitric acid and hydrochloric acid matrices studied.

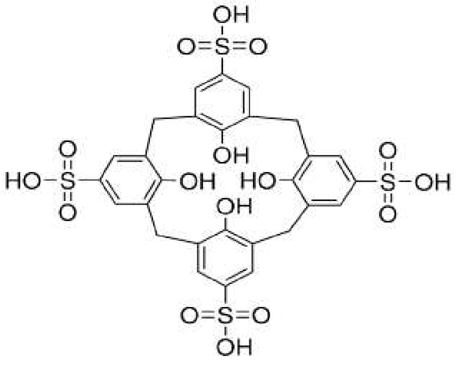

Figure 14. Molecular structure of SC4A

3.5 Batch Studies

The goal of these studies was to investigate how the addition of aqueous extractants would affect the retention of lead by Pb resin. Nitric and hydrochloric acids were used in these experiments, with 7 different nitric acid (HNO_3) concentrations from 0.5 – 10 M and 6 hydrochloric acid (HCl) concentrations ranging from 0.1 – 2 M. The experimental method employed was adapted from several published procedures.[37,45,46]

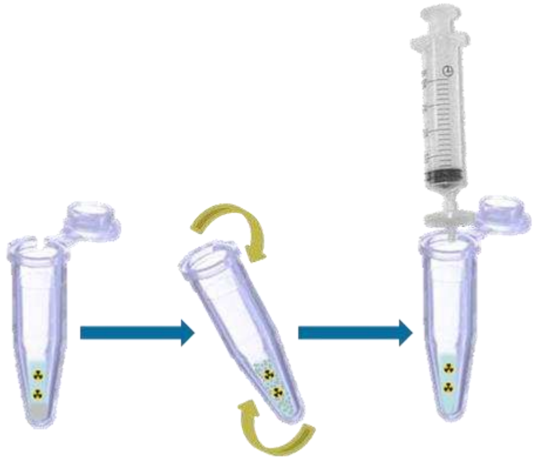

Figure 15. Diagram of batch study procedure

First, a known amount of resin (~10 mg) was placed into a 1.5 mL microcentrifuge tube and preconditioned with 1 mL of the indicated acid by shaking with an Eppendorf ThermoMixer C. The sample was then spiked with a known volume of the ^{212}Pb radiotracer (20 µL) and allowed to equilibrate for 1 hour with mixing. During this interval, each sample was counted by HPGe gamma spectroscopy, and the initial activity was recorded (A_0). After mixing, the sample was filtered into a new microcentrifuge tube through a 0.45 µm Whatman polytetrafluoroethylene (PTFE) filter affixed to a 3 mL polypropylene syringe. Next, a 720 µL aliquot of the filtered solution was transferred to another microcentrifuge tube containing 300 µL of DI water to maintain the same volume as the pre-filtered sample. This aliquoting was done to account for the small loss of solution to the filtration process and a volume correction was applied to the data obtained by next counting the samples by HPGe gamma spectroscopy to determine post-extraction activity (A_s). All samples were prepared in triplicate.

The ^{212}Pb tracer activities in the bulk sample, A_0, and filtrate, A_s, were used to calculate the weight distribution ratio, D_w (Eqn. 1), with A_s adjusted by multiplying the post-extraction activity by the ratio of total volume to aliquot volume (i.e., 1020/720). Equation 2 was used to calculate the number of free column volumes to peak maximum, k', from the D_w. The uncertainty was calculated from the standard deviations of the replicates.

3.5.1 Kinetics Study

The kinetics of extractions using Pb resin in conjunction with a water-soluble calixarene were also explored to determine suitability for a Fl chemical experiment. An HCl concentration with extraction below the maximum ($100 < k' < 1000$, to minimize errors) from the batch experiments was chosen for kinetics studies.[37] First, 10 mg of Pb resin in 1.5 mL microcentrifuge tubes was preconditioned with 1 mL of the specified HCl-calixarene solution at 1000 rpm on a ThermoMixerC for 30 minutes. The resin was then spiked with 20 µL of the ^{212}Pb stock solution and the exact time was recorded to the second (t_0) before being placed back onto the orbital shaker for the specified contact time (5 minutes for standards). After contacting, the sample was filtered into a new 1.5 mL microcentrifuge tube through a 0.45 µm Whatman PTFE filter affixed to a 3 mL polypropylene syringe and the time that the plunger hit the bottom of the syringe was recorded to the second (t_{end}). Finally, a 720 µL aliquot of the filtered solution was transferred to another 1.5 mL microcentrifuge tube containing 300 µL of DI water and counted by HPGe gamma spectroscopy. Standards were prepared without the addition of Pb resin to obtain initial activity values for the samples. In the absence of replicates, uncertainties were calculated using propagation of counting uncertainties.

3.6 Solvent Extraction Studies

The goal of these studies was to investigate the extraction properties of various aqueous and organic extractants. The method employed for SX experiments was adapted from similar studies in the scientific literature.[39,40] To a 1.5 mL microcentrifuge tube containing 500 µL of an organic solvent (with or without organic extractant) 490 µL of acid (with or without extractant) was added. Samples were allowed to pre-equilibrate for 30 minutes on an Eppendorf ThermoMixer C. Next, a 10 µL spike of the radiotracer was added to the centrifuge tubes and the samples were equilibrated for 1 hour on the mixer. A 300 µL aliquot of each phase was removed with a direct displacement pipette and placed into separate microcentrifuge tubes containing DI water to maintain identical volumes. The samples were counted by HPGe gamma spectroscopy, and the activity of ^{212}Pb in each phase was recorded.

Figure 16. Illustrated depiction of the SX procedure

The activities in the aqueous, A_{aq}, and organic phases, A_{org}, were calculated by multiplying the post-extraction activity by the ratio of total volume to aliquot volume. The adjusted activities were used to determine the distribution ratio, D, and percent extracted, %E, using Equations 3 (and/or 4) and 5, respectively. The extraction properties of each system can be visualized by plotting either of these parameters as a function of the varying concentrations. The graphical representation of uncertainty is one standard deviation encompassing only uncertainty from counting statistics.

3.7 HPGe Gamma Spectroscopy

Gamma-ray spectroscopy with high-purity germanium (HPGe) detectors is a very common technique used to identify and determine the activity of radionuclides. The use of HPGe detectors results in much higher-resolution gamma spectra, expressed by the full-width-at-half-maximum (FWHM) of the peaks, than their common counterpart, sodium iodide detectors that are thallium (Tl) activated, NaI(Tl). Many nuclear energy levels that cannot be resolved with a NaI(Tl), such as photo peaks on top of the Compton continuum, can be identified with HPGe detectors due to their increased resolution.[62] In order for a gamma ray to be recorded as an event, it must produce a recoil electron by one of three processes when it enters the detector: photoelectric effect, Compton interaction, or pair production.

In the photoelectric process, all of the energy from the incoming gamma or X-ray is transferred to the recoil electron which then creates electron-hole pairs in the detector. The electron-hole pairs produced in the detector yield an output pulse that is proportional to the energy of the incident gamma or X-ray and appear as full-energy photo peaks in the spectrum. Compton interactions produce a well distributed low-energy area in the spectrum and can be used as a measure of photopeak efficiency. At gamma energies greater than 3 MeV, pair production becomes an important interaction.[63] HPGe detectors are operated at the temperature of liquid nitrogen to limit the number of false signals from electron hole-pair production and collection that arise due to their much higher active volume relative to low-purity detectors. An HPGe gamma-ray spectrometer coupled with a multi-channel analyzer (DSPEC, Ortec) controlled with MAESTRO spectral software (Ortec) was used for all activity measurements presented in this work. All samples and standards were maintained in the same 0.5- or 1-mL geometry so additional efficiency calibrations were not needed.

CHAPTER 4: EXPERIMENTAL RESULTS

4.1 Batch Studies

The extraction of lead by Pb resin was first studied at six HCl concentrations ranging from 0.1 to 2 M, and seven HNO_3 concentrations ranging from 0.5 to 10 M. These concentrations were chosen to mimic the ranges in which lead was extracted by the two acid matrices during the characterization of Pb resin by *Horwitz et al.* and to serve as a baseline for comparison with subsequent batch studies using the resin in combination with calixarenes.[60] Hydrochloric acid concentrations of 0.1, 0.4, 0.8, 1, 1.5, and 2 M, and nitric acid concentrations of 0.5, 1, 2, 4, 6, 8, and 10 M were employed as described in chapter *3.5*. Each acid concentration was replicated in batches of three and the initial (A_0) and post-extraction (A_s) activities of ^{212}Pb measured by HPGe gamma spectroscopy were used to calculate D_w values using Equation 1, which were then converted to k' using Equation 2 with a resin factor of 1.82.[61] The data points shown in the figures below represent the average of the calculated k' values for the triplicates performed at each acid concentration and error bars depict the standard deviation from counting uncertainties of triplicates in each data point.

4.1.1 Eichrom Pb Resin

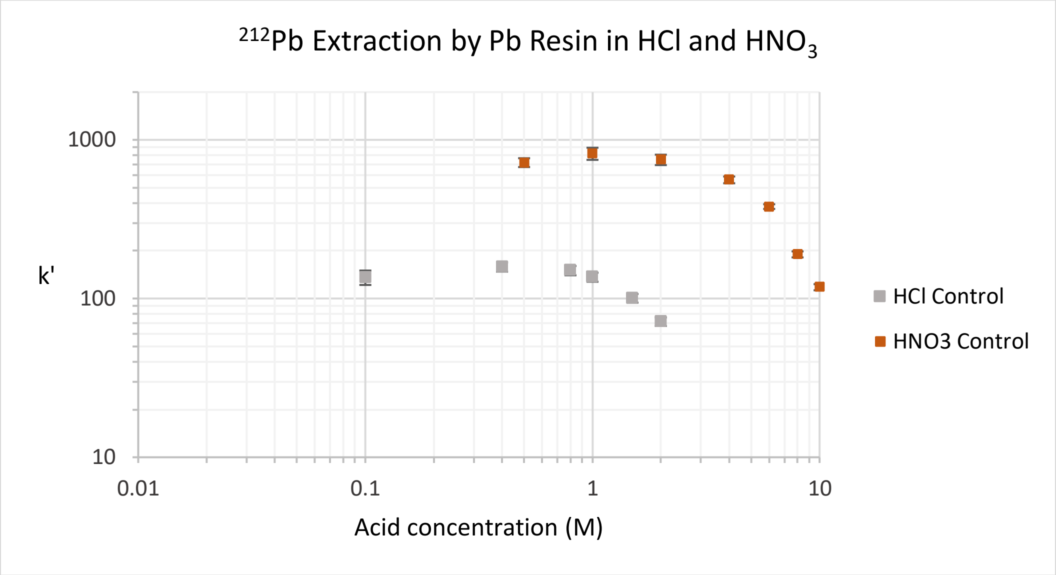

Figure 17. Batch uptake (k’) of ^{212}Pb as a function of acid media on Pb resin (50-100 µm)

Figure 17 shows the trends observed in the uptake of ^{212}Pb by Eichrom Pb resin with increasing concentrations of nitric acid and hydrochloric acid. In hydrochloric acid media, the resin showed increased Pb retention from 0.1 to 0.4 M, where it reached its maximum (k’ = 158.8), followed by a decrease in Pb retention from 0.4 to 2 M. Extraction between 0.4 and 0.8 M HCl overlapped within the error bars. In nitric acid media, uptake of Pb by the resin increased from 0.5 to 1 M, where it reached its maximum (k’ = 822.4), then decreased from 1 to 10 M HNO_3. The relatively small error bars indicate good agreement in calculated uncertainty between replicates.

4.1.2 Eichrom Pb resin with 4-Sulfocalix[4]arene

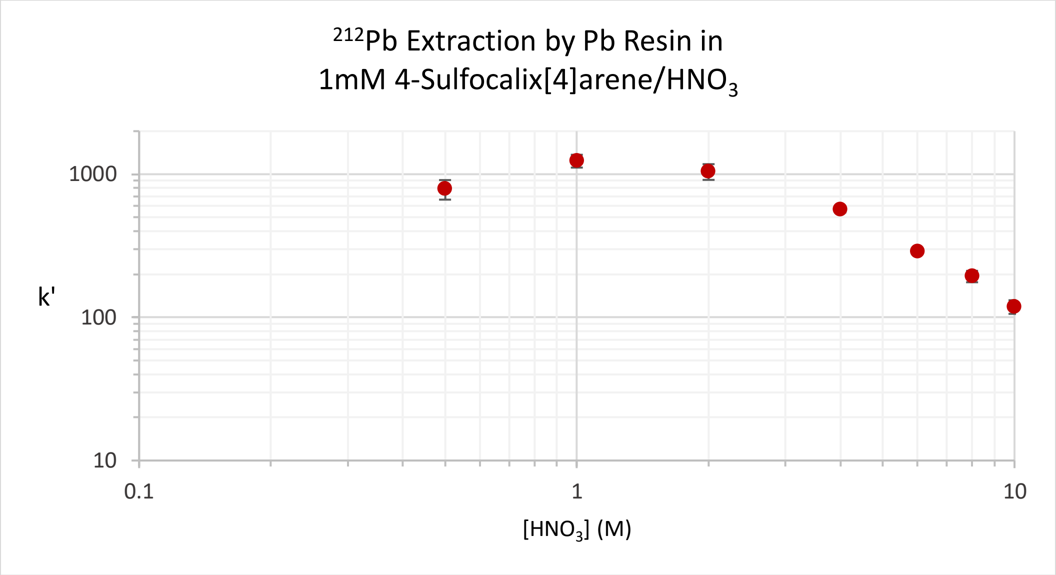

Figure 18. Batch uptake (k’) of ^{212}Pb by Pb resin from varying nitric acid media containing 1 mM SC4A

Figure 18 shows the trends observed in the uptake of ^{212}Pb by Eichrom Pb resin from nitric acid media all containing 1 mM of 4-Sulfocalix[4]arene dissolved in increasing concentrations of HNO_3. Lead retention by the resin increased from 0.5 to 1 M, where it reached its maximum (k’ = 1140.5), followed by a steady decrease in retention up to 10 M HNO_3. The small error bars (all are included, though some do not exceed area of data points) indicate good agreement in calculated uncertainty between replicates, with no overlap between concentrations.

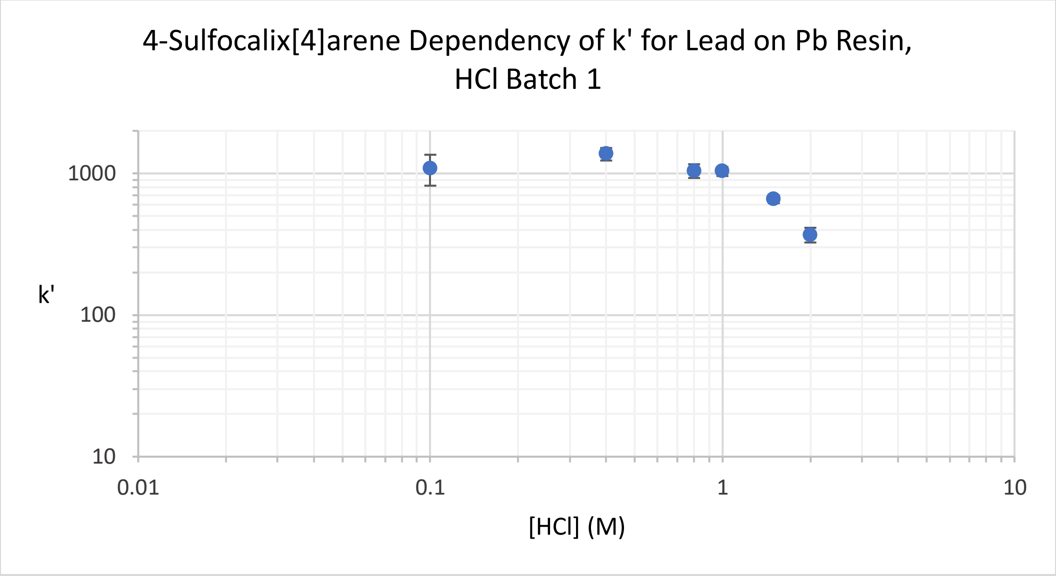

Figure 19. Batch 1 uptake (k’) of ^{212}Pb by Pb resin from varying hydrochloric acid media containing 1 mM SC4A

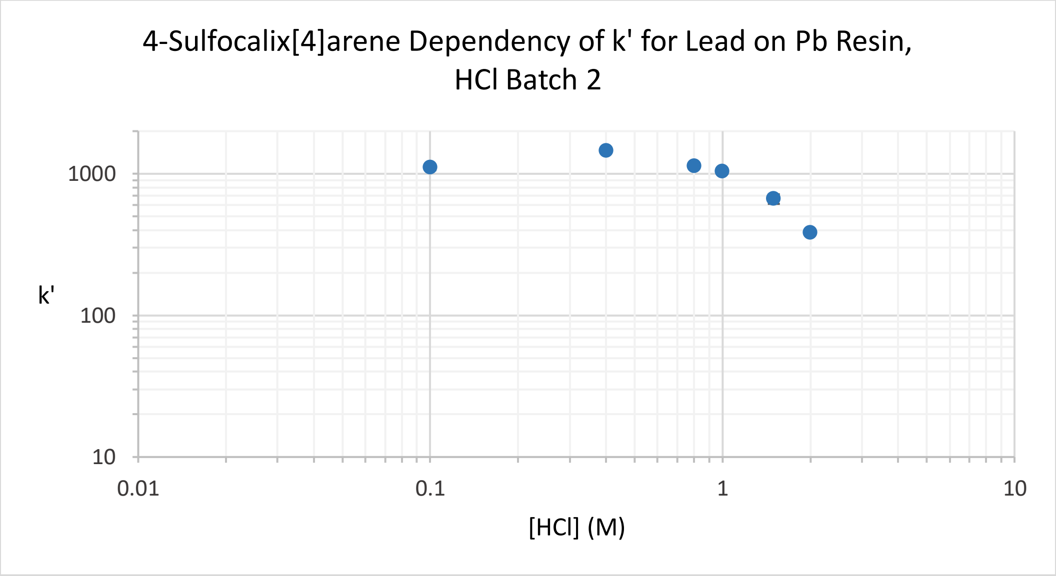

Figure 20. Batch 2 uptake (k’) of ^{212}Pb by Pb resin from varying hydrochloric acid media containing 1 mM SC4A

As shown in Figures 19 and 20, a very efficient separation of ^{212}Pb by Pb resin from hydrochloric acid media containing 1 mM of 4-Sulfocalix[4]arene was obtained. The batch study was repeated due to the surprising nature of the results, which will be discussed in Chapter 5. Lead retention by the resin in hydrochloric acid media increased from 0.1 to 0.4 M, where it reached its maximum ($k'_{average}$ = 1460.2), followed by a decrease to overlapping values at 0.8 and 1 M, and then a steady decrease up to 2 M HCl. The error bars represent the standard deviation between replicates and in some cases do not exceed the size of the data points. Comparison of the uncertainties indicates good agreement between replicates and between batches.

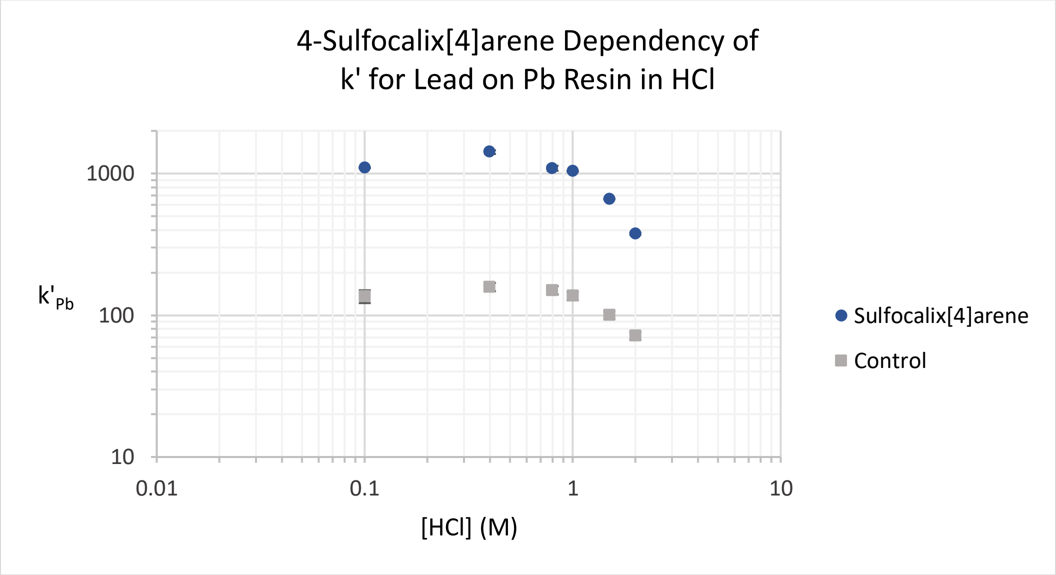

Figure 21. Comparison of the batch uptake (k') of ^{212}Pb by Pb resin from hydrochloric acid media in the presence and absence of SC4A

A comparison of the data shown in Figure 17 with the averaged data from Figures 19 and 20 is presented above (*fig.21*). The trends in the uptake of ^{212}Pb by Eichrom Pb resin (50 – 100 µm) in hydrochloric acid media are the same for both systems, regardless of 4-Sulfocalix[4]arene content: Pb retention increases from 0.1 to 0.4 M HCl, then decreases to an overlapping degree in both 0.8 and 1 M HCl, followed by a continual decrease up to 2 M HCl. The relative size of the error bars indicated good experimental precision between replicates and there is no overlap in extraction between the two systems.

4.1.2.1 Kinetics Study

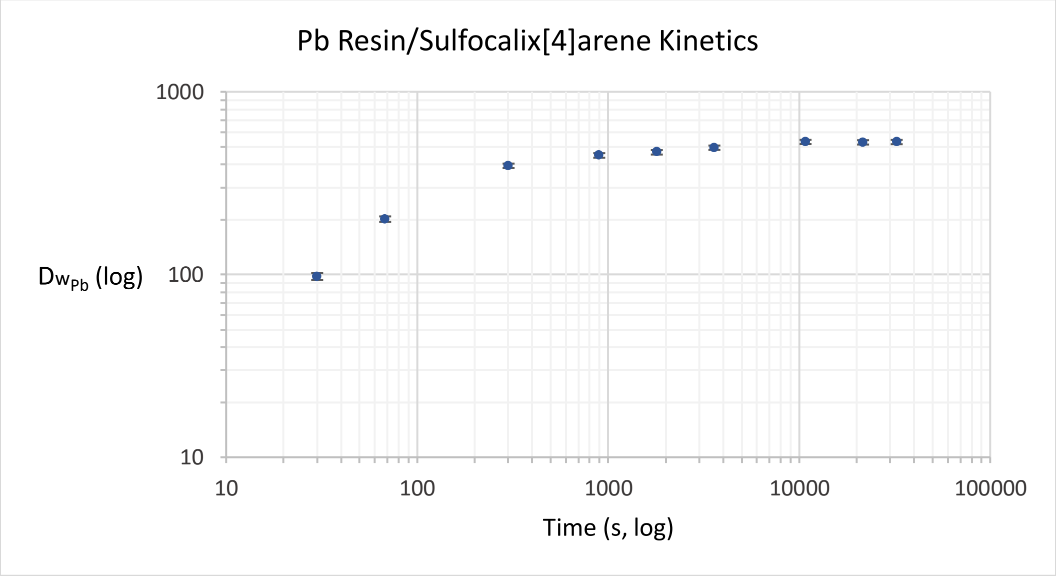

Figure 22. Uptake (D_w) of ^{212}Pb by Pb resin from 1 mM SC4A in 1M HCl as a function of time

Finally, a kinetics study was performed with the Pb resin/SC4A system in hydrochloric acid media to determine the feasibility of pursuing a SX study with the extractant coated to Eichrom's Pb resin. Figure 22 shows trends in the uptake of ^{212}Pb by Pb resin from 1 M HCl containing 1 mM 4-sulfocalix[4]arene as a function of contact time. The weight distribution, D_w, after thirty seconds of contact time is already >97 and lead extraction effectively levels off after three hours (D_w = 531.46). Replicates were not performed due to time constraints and the error bars represent uncertainty from counting statistics.

4.2 Solvent Extraction Studies

The extraction of lead by various organic extractants was studied in SX systems using hydrochloric acid as the aqueous phase at 16 concentrations: 0.01, 0.02, 0.03, 0.04, 0.06, 0.08, 0.1, 0.2, 0.4, 0.8, 1, 2, 4, 8, 10, and 10.8 M. A broad range of HCl concentrations between 0.01 and 1 M was chosen to elucidate the higher extraction behaviors expected from very dilute systems. For studies with HT18C6 and DBHT18C6, the organic phase consisted of carbon tetrachloride (CCl_4) containing 10^{-4} M thiacrown ether, the maximum concentration possible due to the very low solubility of these macrocyclic extractants in organic solvents. For studies with calixarenes, the organic phase consisted of chloroform ($CHCl_3$) containing 10^{-3} M C4A, TC4A or SO_2CA. These concentrations were chosen taking into account the abundance of each extractant relative to ^{212}Pb added to the system along with their solubilities in each organic solvent. Liquid-liquid separations at each aqueous HCl concentration were performed in triplicate and the data points shown on the following figures represent the averaged values of the calculated distribution ratios, D, for the replicates.

4.2.1 Thiacrown Ethers

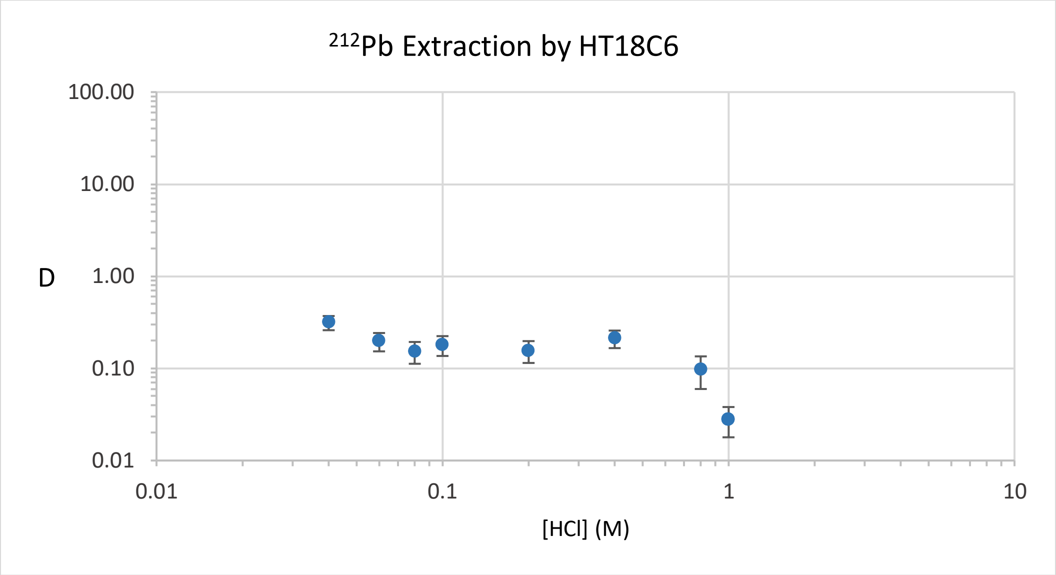

Figure 23. Uptake (D) of ^{212}Pb by 0.1 mM HT18C6 in CCl_4 as a function of HCl concentration

Figure 23 shows the trends observed in the uptake of ^{212}Pb by 10^{-4} M hexathia-18-crown-6 in CCl_4 from hydrochloric acid media. HCl concentrations in the thiacrown ether studies ranged from 0.04 to 10.8 M in an effort to independently verify values in the literature.[46] Lead extraction peaked in 0.04 M HCl, and no extraction was observed at HCl concentrations exceeding 1 M. The data point at 0.04 M HCl corresponds to a D-value of 0.32, or 23.9% ^{212}Pb extracted. The error bars represent the standard deviation of uncertainty between replicates and there is significant overlap between the data points at 0.06 and 0.8 M HCl.

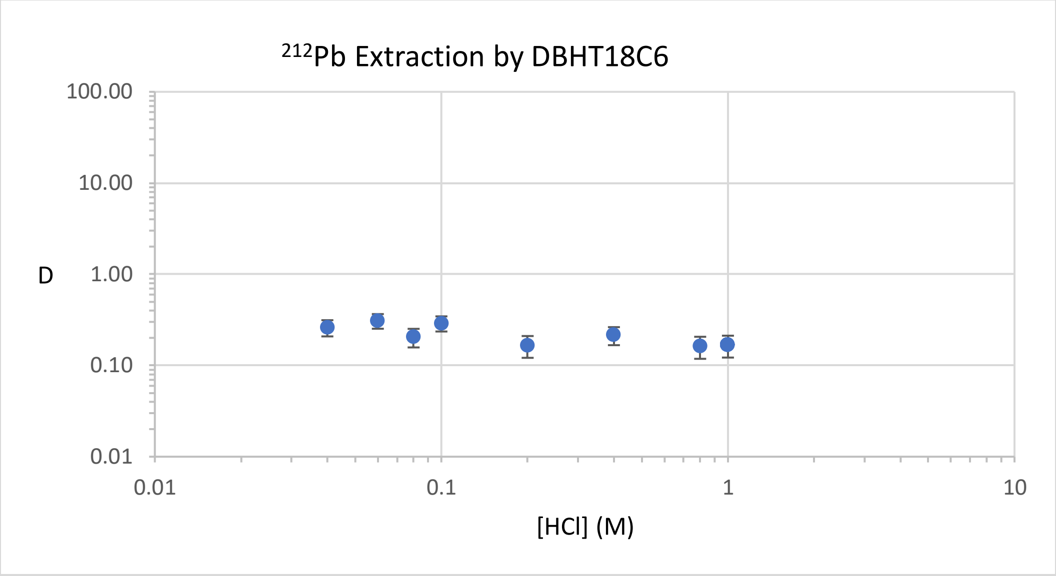

Figure 24. Uptake (D) of ^{212}Pb by 0.1 mM DBHT18C6 in CCl_4 as a function of HCl concentration

Figure 24 shows the trends observed in the uptake of ^{212}Pb by 10^{-4} M dibenzo-hexathia-18-crown-6 in CCl_4 from hydrochloric acid media. As can be seen, similar behavior was observed for lead as in Figure 23, with no extraction whatsoever above 1 M HCl. The error bars represent the standard deviation of uncertainty amongst replicates and there is a significant overlap between the data points for 0.04 and 1 M HCl. The highest distribution ratio from this dataset is D = 0.31, which corresponds to 23.4% extracted. Because the distribution ratios calculated for samples in 2 to 10.8 M HCl were equivalent to zero, limits were set at or near D = 0.01 by calculating distribution ratios based on background counts in the aqueous or organic phase (whichever was fundamentally zero) over the counting duration.

4.2.2 Calixarenes

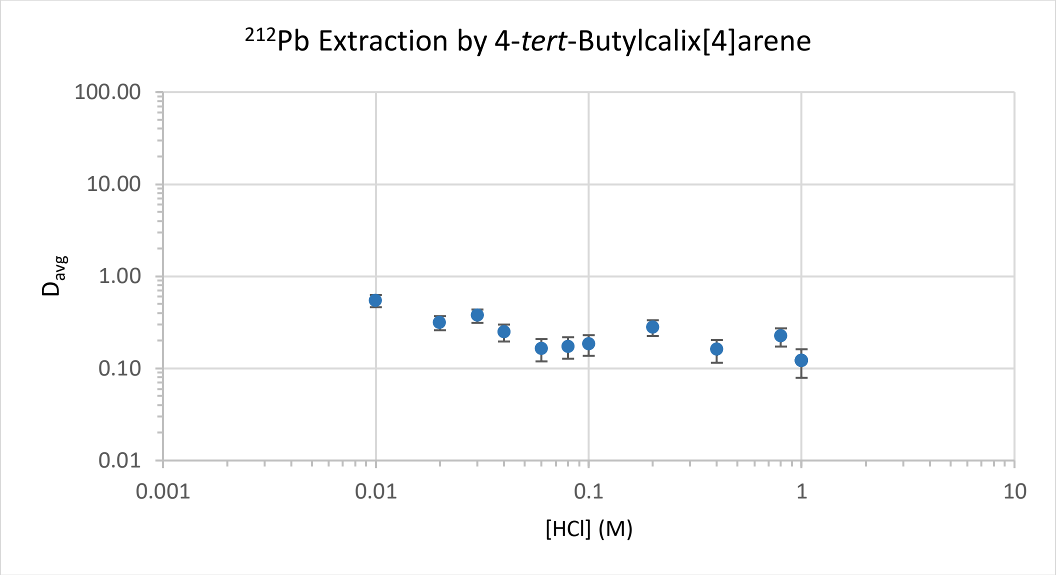

Figure 25. ^{212}Pb extraction by 1 mM C4A in $CHCl_3$ from hydrochloric acid media

The extraction of lead by 4-*tert*-butylcalix[4]arene (C4A), the methylene-bridged structure all of the sulfur-bridged calix[4]arenes in this study are based on, was studied as a baseline to which extraction by its sulfur analogs could be compared (Chapter 5). Figure 25 shows the trends observed in the uptake of ^{212}Pb by 1 mM C4A in $CHCl_3$ from hydrochloric acid media. Extraction peaked in 0.01 M HCl with a distribution ratio of 0.54 (34.9% extracted), and no extraction occurred above 1 M HCl. The error bars represent the standard deviation of uncertainty between replicates and there is a significant overlap between the data points for 0.02 to 0.04 M, 0.06 to 0.1 M, and 0.4 and 1 M HCl.

4.2.2.1 4-*tert*-Butylthiacalix[4]arene

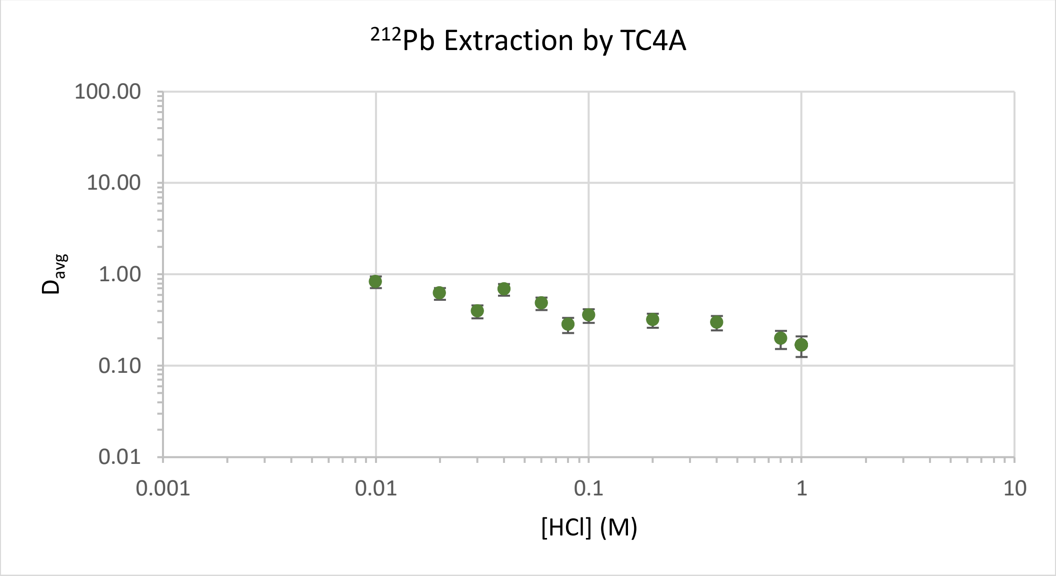

Figure 26. ^{212}Pb extraction by 1 mM TC4A in $CHCl_3$ from hydrochloric acid media

Figure 26 shows the trends observed in the uptake of ^{212}Pb by 1 mM 4-*tert*-butylthiacalix[4]arene in $CHCl_3$ from hydrochloric acid media. Lead extraction by TC4A peaked in 0.01 M HCl with a distribution ratio of 0.83 (44.3% extracted), and no extraction was observed at HCl concentrations exceeding 1 M. The error bars represent the standard deviation of uncertainties between replicates and overlap can be seen following trends similar to those in Figure 25.

4.2.2.2 4-*tert*-Butylsulfonylcalix[4]arene

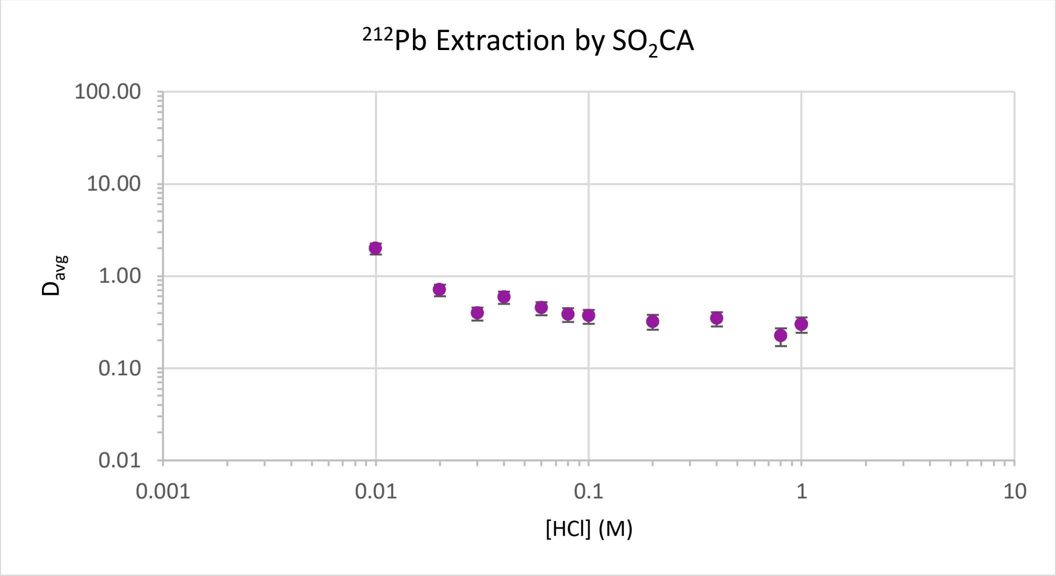

Figure 27. ^{212}Pb extraction by 1 mM SO_2CA in $CHCl_3$ from hydrochloric acid media

Figure 27 shows the trends observed in the uptake of ^{212}Pb by 1 mM 4-*tert*-butylsulfonylcalix[4]arene in $CHCl_3$ from hydrochloric acid media. Lead extraction by SO_2CA peaked at 0.01 M HCl with a distribution ratio of D = 1.99 (66.1% extracted), followed by an overall decrease with increasing HCl concentration up to 1 M with no extraction observed above 1 M HCl. The error bars represent the standard deviation of uncertainty between replicates and overlap can be seen for the data points between 0.03 and 1 M HCl.

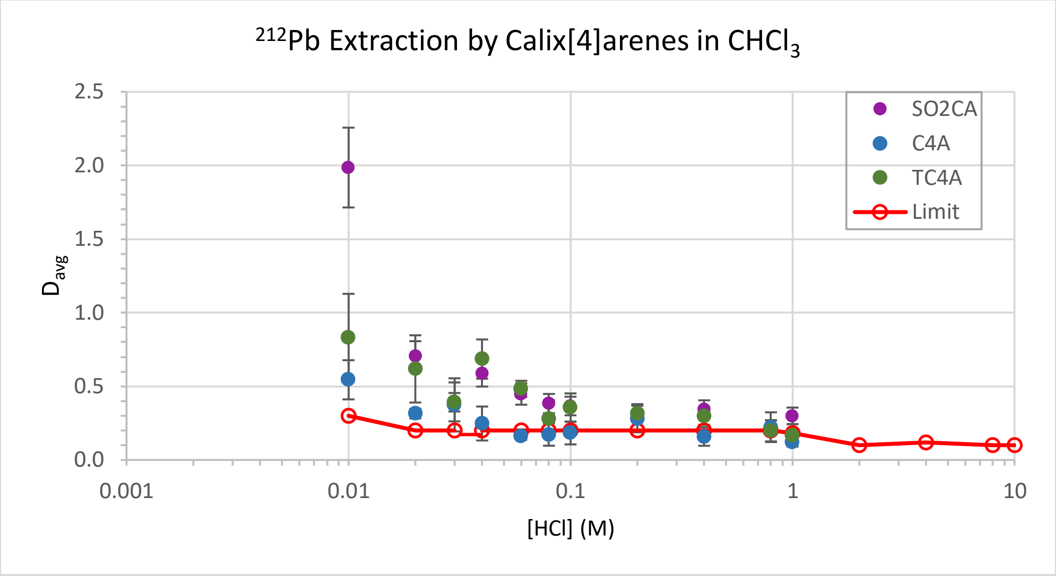

Figure 28. ^{212}Pb extraction by various calix[4]arenes in $CHCl_3$ from hydrochloric acid media, with limits

Figures 25, 26, and 27 are summarized above in Figure 28, which shows the trends observed in the uptake of ^{212}Pb by 1 mM of the indicated calix[4]arene in $CHCl_3$ from hydrochloric acid media along with an analytical limit. The limits were set by calculating distribution ratios based on background counts over the counting duration. Figure 28 shows that the greatest lead uptake occurred in 0.01 M HCl for all three calix[4]arenes in the order SO_2CA > TC4A > C4A with distribution ratios of 1.99 ± 0.27, 0.83 ± 0.29 and 0.54 ± 0.13, respectively. Taking the limits into account, the only data considered in the discussion (Chapter 5) will be: SO_2CA from 0.01 to 1 M HCl, TC4A from 0.01 to 0.4 M HCl, and C4A from 0.01 to 0.03 M HCl.

4.2.3 Crown Ether 4’,4”(5”)-di-*tert*-butyldicyclohexano-18-crown-6

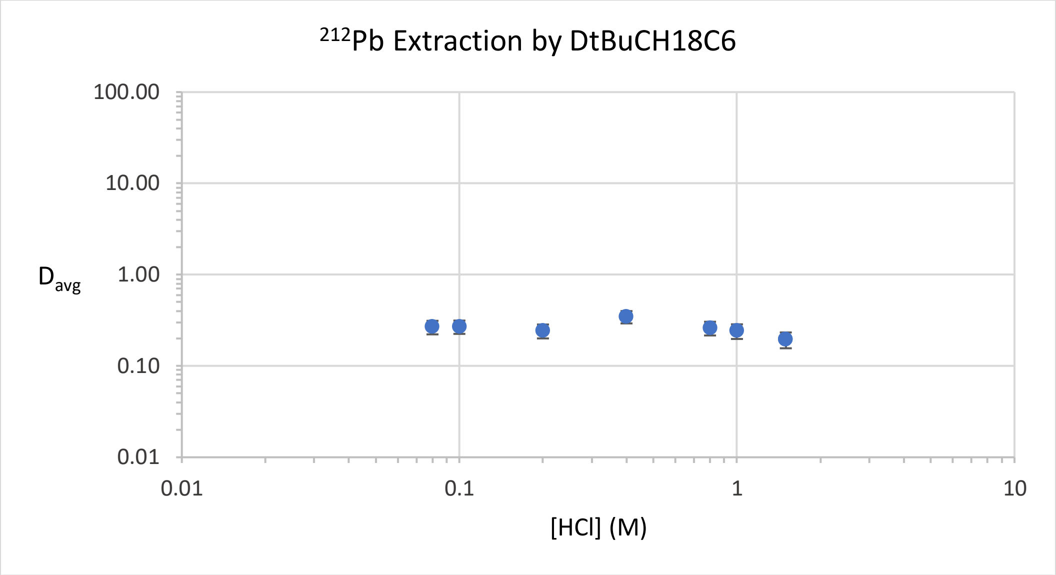

Figure 29. Uptake (D) of ^{212}Pb as a function of HCl concentration by 0.01 M DtBuCH18C6 in CCl_4

Figure 29 shows the trends observed in the uptake of ^{212}Pb by 0.01 M 4’,4”(5”)-di-*tert*-butyldicyclohexano-18-crown-6 in CCl_4 from hydrochloric acid media. This data was obtained for the purpose of selecting an optimal HCl concentration for use in all subsequent SX experiments with DtBuCH18C6. Lead extraction peaked at 0.4 M HCl with a distribution ratio of 0.35 (25.5% extracted). Error bars in the figure represent the standard deviation of uncertainty between replicates, which are shown to be in good agreement.

4.2.3.1 Speciation Study

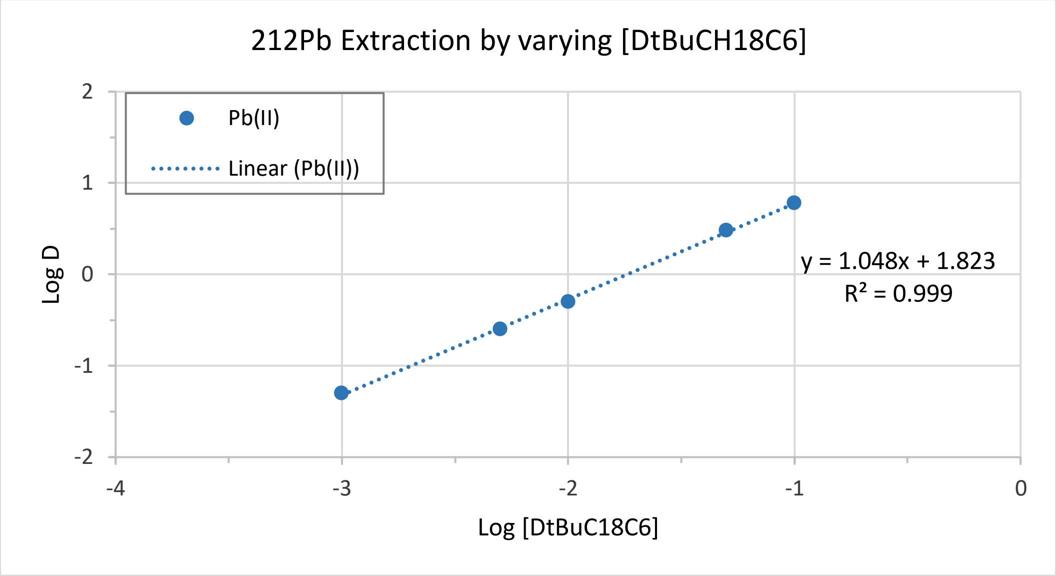

Figure 30. Extraction of $^{212}Pb^{2+}$ as a function of DtBuCH18C6 concentration

Figure 30 shows the distribution ratios for the extracted ^{212}Pb(II) by 0.001, 0.005, 0.01, 0.05, and 0.1 M 4′,4″(5″)-di-*tert*-butyldicyclohexano-18-crown-6 in CCl_4 from 0.4 M HCl. The linear regression (dotted line) indicates that the number of DtBuCH18C6 ligands coordinated to the Pb(II) metal ion is 1.05, therefore the reaction stoichiometry is 1:1. The maximum lead extraction is seen in 0.1 M DtBuCH18C6 with a distribution ratio of 6.01, which corresponds to 85.7% of the ^{212}Pb extracted.

4.2.3.2 4',4"(5")-di-*tert*-butyldicyclohexano-18-crown-6 with 4-sulfocalix[4]arene

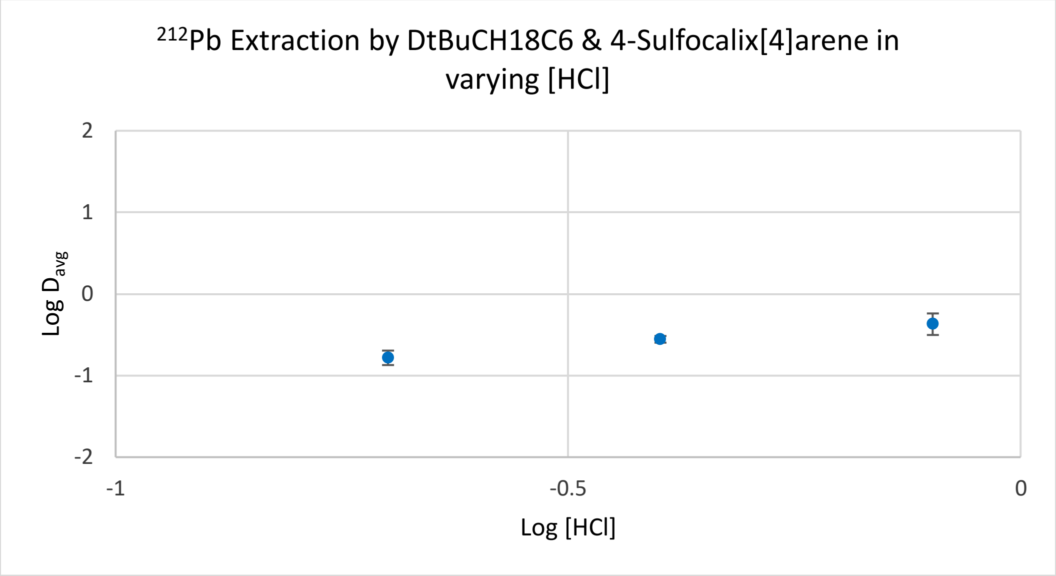

Figure 31. Extraction of ^{212}Pb by 0.06 M DtBuCH18C6 from hydrochloric acid media containing 1 mM SC4A

Figure 31 shows the extraction of ^{212}Pb by 0.06 M 4',4"(5")-di-*tert*-butyldicyclohexano-18-crown-6 in CCl_4 from varying concentrations of HCl containing 1 mM of 4-sulfocalix[4]arene as an additional complexing agent. Lead extraction was shown to increase with increasing HCl concentration with the maximum distribution ratio (D = 0.43) occurring in 0.8 M HCl. The error bars represent the standard deviation of uncertainties between replicates at each HCl concentration and the data points at 0.4 and 0.8 M HCl overlap.

CHAPTER 5: DISCUSSION

5.1 Batch Studies

Data obtained from the batch distribution studies in Chapter 4 helped to elucidate the effects of acid concentration and complexant availability in the mobile phase on the uptake of ^{212}Pb by Eichrom Technologies' Pb resin. By combining the data collected as part of this work with data previously reported by *Horwitz et al.*, trends can be summarized regarding the uptake of lead from both nitric acid and hydrochloric acid matrices that are useful for comparison to the novel system containing an additional complexing agent studied herein.

5.1.1 Pb Resin Comparison to Prior Data

In preliminary experiments, batch distribution studies with Pb resin in nitric acid and hydrochloric acid media were conducted for comparison to the literature and in order to establish a baseline of ^{212}Pb retention by the resin across a range of concentrations. The data collected in this work, as shown in Figure 17, was in very good agreement (*fig.32*) with the capacity factors (k') published by *Horwitz et al.*, shown in Figure 12.[60] This served as validation of both the experimental procedure and the observed trends in ^{212}Pb extraction by Pb resin from 0.5 to 10 M HNO_3 and 0.1 to 2 M HCl which were then utilized to interpret the data obtained in subsequent experiments with Pb resin.

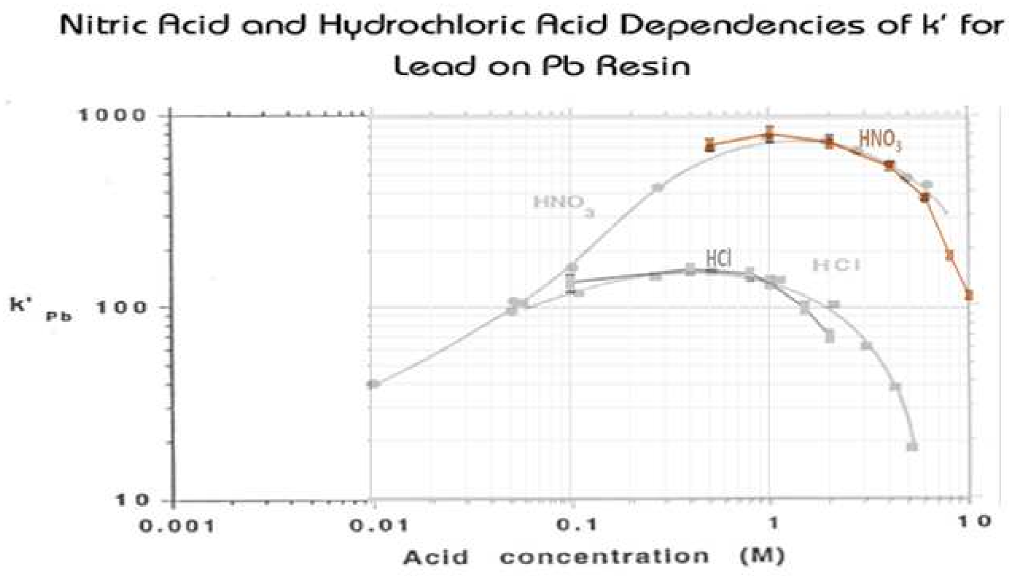

Figure 32. Comparison of data from Figures 12 and 17

5.1.2 Pb Resin with 4-Sulfocalix[4]arene

Following the characterization of Pb resin above, the same analytical method was used in batch studies with the resin in nitric acid and hydrochloric acid matrices containing 1 mM concentrations of 4-sulfocalix[4]arene. SC4A was the only water-soluble calixarene studied in this work, and the motivation behind these studies was to evaluate whether it displayed a competitive affinity for lead over a known lead extractant for potential use in a SX system. The data obtained for the nitric acid system containing 1 mM SC4A (*fig.18*) can be evaluated in direct comparison to the respective control data (*fig.17*) as shown in Figure 33.

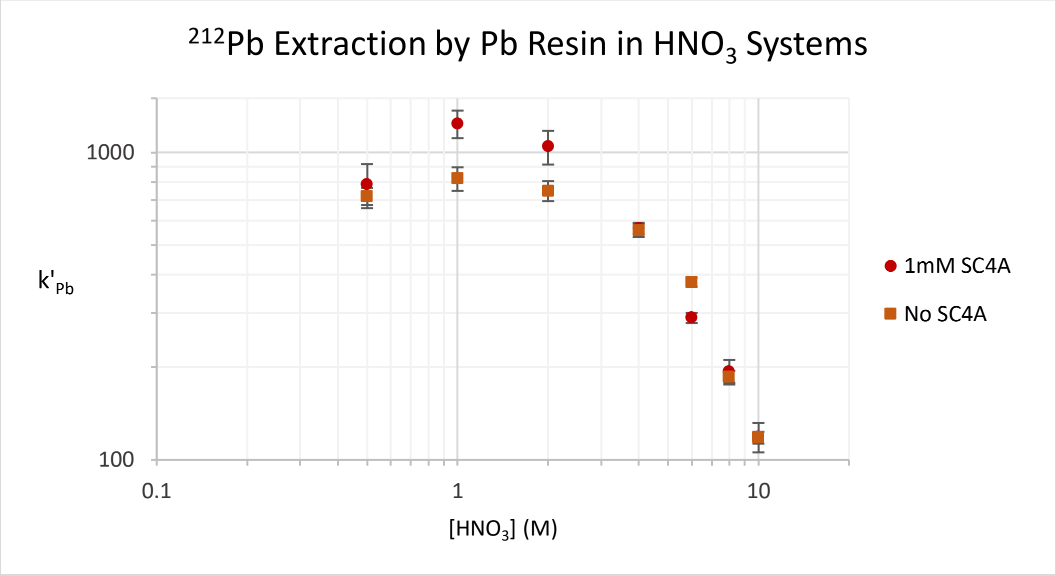

Figure 32. Comparison of the batch uptake (k’) of ^{212}Pb by Pb resin in nitric acid media in the presence and absence of SC4A

Lead extraction by the Pb resin/HNO_3 system containing SC4A was greater than that observed by Pb resin alone. These results indicate that 4-sulfocalix[4]arene does not extract ^{212}Pb more competitively than the lead-selective extraction chromatographic resin. Instead, a very mild synergistic effect was observed from 1 and 2 M HNO_3, which exhibited an approximately 150% increase in Pb adsorption to the stationary phase. Chemical separations in nitric acid media were not pursued any further.

5.1.2.1 Pb Resin with 4-Sulfocalix[4]arene in HCl

When the data from the initial batch study with Pb resin in hydrochloric acid matrices containing SC4A, “Batch 1”, was analyzed and plotted (*fig.19*), a significant deviation from the control study (*fig.17*) was immediately apparent. This system showed, on average, more than a seven-fold increase in ^{212}Pb retention by the resin across the entire HCl concentration range.

The batch experiment was repeated, “Batch 2”, in order to confirm the profound synergistic effect observed (*fig.20*). The data obtained from both batch studies was determined to be in agreement and the average k’ values were compared to the respective control, presented in Figure 21. In 0.4 M HCl, extraction of ^{212}Pb by the system containing 1 mM SC4A surpassed the control system by nearly an order of magnitude ($k'_{HCl\text{-}SC4A}/k'_{HCl}$ = 9.22). This indicates that SC4A forms complexes with Pb^{2+} ions very efficiently in the mobile phase and the organic extractant on Pb resin is more selective for the lead complex, a notion supported by the knowledge that adsorption of a metal ion in EXC entails the conversion of hydrated metal ions into neutral complexes with affinity for the organic extractant. These results inspired all subsequent studies involving 4-sulfocalix[4]arene presented in this work.

5.1.2.1.1 Pb resin/4-Sulfocalix[4]arene Kinetics Study

Following the success of the experiments discussed in *5.1.2.1,* the feasibility of the system was investigated as a potential candidate for application in solvent extraction studies. Since it is already known that neither EXC with Pb resin nor SX with 4’,4”(5”)-di-tert-butyldicyclohexano-18-crown-6, the organic extractant coated onto Pb resin, alone are capable of achieving kinetics fast enough to be suitable for TAN experiments, it was necessary to evaluate the extraction kinetics of the Pb resin/SC4A system before a budget would be approved to order the materials necessary to study the system via SX.[46]

The kinetics study was carried out in 1 M HCl because maximum ^{212}Pb extraction achieved at lower concentrations was sufficiently high to be associated with larger uncertainties. Even under suboptimal conditions, Figure 22 shows that the shortest contact time, 30 s, yields efficient extraction of lead, making this system the best candidate for further development. While this study indicates that Pb would not be at full equilibrium on the second time scale required of a Fl experiment, Pb extraction sufficient to reach an equilibrium-like state is attainable in a matter of seconds. Subsequently, a SX system was designed utilizing the crown ether found on Pb resin, DtBuCH18C6, as the organic extractant with CCl_4 as the organic diluent and SC4A in HCl matrices as the aqueous phase.

5.2 Solvent Extraction Studies

5.2.1 Thiacrown Ethers

Thiacrown ethers are not commercially available and are notoriously difficult to produce as their synthesis route uses HD mustard. The unique capabilities at Lawrence Livermore National Laboratory's Forensic Science Center made the synthesis of these macrocycles possible. This provided the rare opportunity to independently verify literature studies with the thiacrown ethers hexathia-18-crown-6 and dibenzo-hexathia-18-crown-6.

5.2.1.1 Comparison to Prior Data

The SX extraction study with HT18C6 (*fig.23*) yielded distribution ratios all below 1, which do not exceed detection limits comparable to literature values (*fig.8*).[44,46] The uptake of ^{212}Pb by DBHT18C6 reported in this work (*fig.24*) is also comparable to the literature (*fig.9*), with distribution ratios at or below calculated detection limits.[45] This supports the published authors' interpretation that neither HT18C6 nor DBHT18C6 extract lead.

5.2.2 Calixarenes

Three calix[4]arenes were evaluated as organic extractants for the separation of ^{212}Pb from hydrochloric acid matrices via solvent extraction. The calixarenes 4-*tert*-butylcalix[4]arene, 4-*tert*-butylthiacalix[4]arene, 4-*tert*-butylsulfonylcalix[4]arene, and 4-*tert*-butylsulfinylcalix[4]arene were identified as potential extractants for soft metals including Pb from the literature.[51,58,64,65] C4A, TC4A, and SO_2CA were ultimately selected for investigation due to their commercial availability. The data generated in this work was intended to be used to evaluate the feasibility of incorporating one of these macrocycles with a crown ether into a novel calixcrown for future study by the research group at LLNL.

Extraction of ^{212}Pb was low for each calixarene from 0.04 to 1 M HCl and non-existent from HCl matrices above 1 M, so additional experiments were carried out for lead in 0.01, 0.02, and 0.03 M HCl. The best extractions occurred from hydrochloric acid matrices below 0.04 M and the distribution ratios for each system increased with decreasing acid concentration. Overall, extractions were too low to justify kinetics studies. The selectivity of ^{212}Pb extraction by the SX systems decreased in the order SO_2CA > TC4A > C4A. This indicates that the binding ability and selectivity of calix[4]arenes for lead can be improved by replacing the methylene bridges with sulfur and by changing the oxidation states of the bridging sulfur. The implication is that modification of the bridging sulfurs in thiacalixarenes introduces the possibility of further functionalization at the bridge positions, for example through the incorporation of a polyether loop (e.g., crown ether) on the lower rim.

5.2.3 4’,4”(5”)-di-*tert*-butyldicyclohexano-18-crown-6

A SX study with DtBuCH18C6 and HCl without SC4A (*fig.29*) was carried out to reproduce studies in the literature and form a basis for comparison with systems containing SC4A. It was confirmed that DtBuCH18C6 at low concentrations does not extract Pb. As this was the first study with an unopened bottle of DtBuCH18C6 in this work, it did however provide useful insight into best practices for the preparation of organic phase stock solutions going forward. DtBuCH18C6 comes from the manufacturer in “solid” form, but it is extremely hygroscopic and rapidly becomes a semi-solid once the bottle is opened. This semi-solid state renders it difficult to handle and its mass will fluctuate as it absorbs moisture from the air. These difficulties were overcome by gently melting the crown ether until it became liquid and then using a pipet to transfer it for weighing. As a liquid, the varying amounts of crown ether were diluted to the desired volume using volumetric flasks.

5.2.3.1 Speciation with 4’,4”(5”)-di-*tert*-butyldicyclohexano-18-crown-6

Chemical speciation of the extracted complex was determined by calculating the distribution ratio at varying concentrations of DtBuCH18C6 in the organic phase. The logarithm of the distribution ratios for $^{212}Pb^{2+}$ was plotted as a function of the logarithm of the concentration of DtBuCH18C6 in Figure 30. Applying a linear fit to the data points yields a slope of approximately 1, indicating a 1:1 reaction stoichiometry. This means that one DtBuCH16C6 molecule is required to extract one $^{212}Pb^{2+}$ ion into the organic phase, supporting the conclusion that Pb^{2+} extracts into the cavity of the crown ether and yielding the extraction mechanism:

$$PbCl_{2\,aq} + DtBuCH18C6_{org} \rightleftharpoons PbCl_2 \cdot DtBuCH18C6_{org}$$

5.2.4 4’,4”(5”)-di-*tert*-butyldicyclohexano-18-crown-6 with 4-sulfocalix[4]arene

With the $^{212}Pb^{2+}$ extraction mechanism by DtBuCH18C6 known, the next step was to add SC4A to the aqueous phase of the solvent extraction system. Batch studies with Pb resin and SC4A in HCl showed that the highest lead extraction occurred from 0.4 M HCl, so concentration ranges below, at, and above 0.4 M HCl were chosen in order to confirm the trends from batch studies. Surprisingly, ^{212}Pb extraction was extremely low across the entire range of concentrations, whereas SC4A significantly improved extraction by DtBuCH18C6 coated to the resin in EXC studies. This serves as an excellent example of how EXC data can provide a useful – but never quantitative – guide to the design of SX systems, and vice versa.

CHAPTER 6: CONCLUSION

6.1 Overview

The aim of this research was to investigate two classes of macrocyclic extractants for their potential use in a chemical separation system that could ultimately be applied to the first chemical study of Fl in the aqueous phase. Crown ethers and calixarenes were evaluated as extractants for Pb, a Group 14 homolog of Fl. Due to increasingly strong relativistic effects in the superheavy TANs, the placement of Fl on the Periodic Table has been called into question by conflicting predictions of its chemical properties relative to those of its lighter homologs. Because of the low production rates and short half-lives of Fl isotopes, a chemical system that is both extremely fast and highly selective for Pb at the ultra-trace scale will need to be developed in order to perform a Fl experiment and conclusively determine its aqueous chemical behavior.

6.2 Batch Studies

Eichrom Pb EXC resin, containing the known Pb extractant DtBuCH18C6, was used in all batch studies. Previous studies demonstrated good extraction of ultra-trace carrier-free Pb radionuclides using Pb resin, though kinetics proved to be too slow for a Fl experiment. The extraction of ^{212}Pb by Pb resin in the presence of SC4A was evaluated through batch studies in both nitric and hydrochloric acid. It was found to be enhanced compared to uptake by the resin itself by a factor of 9 in HCl. Kinetic studies revealed that Pb reached extraction equilibrium in approximately 5 minutes. These SC4A/HCl studies with Pb resin indicated that rapid, efficient separations of Fl homologs could be achieved, and an analogous SX system was consequently designed for further investigations.

6.3 Solvent Extraction Studies

SX systems utilizing the thiacrown ethers HT18C6 and DBHT18C6 in CCl_4 as the organic phase were studied and neither was shown to extract Pb from HCl matrices, which is in agreement with previous studies. Three unsupported calixarenes in $CHCl_3$ as the organic phase were shown to extract Pb from very dilute HCl matrices in the order C4A < TC4A < So_2CA, indicating that the selectivity of calix[4]arenes can be manipulated via functionalization of the bridging atoms. The crown ether DtBuCH18C6, the extractant coated to the Pb resin used above, was used as the organic extractant with CCl_4 as diluent in studies with HCl and exhibited negligible Pb extraction. The results of a speciation study revealed that extraction of $^{212}Pb^{2+}$ by DtBuCH18C6 occurs through the formation of a 1:1 complex in the cavity of the crown ether. SC4A was added to the aqueous phase of the SX system containing the organic extractant DtBuCH18C6 in CCl_4 and failed to extract Pb from the same HCl matrices that yielded extremely high uptake in the comparable EXC system.

6.4 Future Work

Due to the lower-than-anticipated Pb extraction trends exhibited by the calixarenes C4A, TC4A and SO_2CA in $CHCl_3$, it would be worthwhile to repeat the SX experiments with CCl_4 (no donor atoms, no hydrogen bond-forming capabilities) as the organic phase in order to minimize phase carry over, which can significantly affect results in trace level experiments with microliter volumes. Further, SX studies with 4-tert-butylsulfinylcalix[4]arene (SOCA), possessing different functionalization at the bridge positions than SO_2CA, should be carried out once the synthesis that was started as a side-project during this work is complete.

The use of crown and thiacrown ethers as extractants in Fl homolog studies should not be written off just because HT18C6, DBHT18C6 and DtBuCH18C6 on their own do not extract Pb, and neither should the thiacalixarenes. It was shown that the selectivity of calixarenes is due to the presence of the cavity (C4A, TC4A, SO_2CA) as well as due to the outer functional groups (SC4A). The implication is that the bridging sulfurs in thiacalixarenes not only change the cavity dimension (elongated C–S bonds), but also introduce the possibility for further functionalization at the bridge positions; for example, by incorporating a polyether loop (i.e., crown ether) on the lower rim of the calix[4]arene.[64] Trends in Pb selectivity observed for the crown ethers and calixarenes in this work can be used to inform the design of novel calixcrown extractants.

Observations of Pb extraction in the novel EXC system combining Pb resin with a mobile phase containing 4-Sulfocalix[4]arene presented in this work have significant implications for its potential implementation in a Fl experiment. The SX system, however, will require further development. The discrepancy in Pb extraction between the EXC and SX systems containing the organic extractant DtBuCH18C6 and aqueous SC4A warrants further investigation. Since a significant decrease in extraction occurred upon the addition of SC4A to the SX system's aqueous phase, the first step would be to determine whether this is the result of an interaction between SC4A and the organic diluent. This can be evaluated by performing SX experiments with SC4A in HCl as the aqueous phase and only CCl_4 as the organic phase.

REFERENCES

1. Pyykko P, Desclaux JP (1979). Relativity and the periodic system of elements. *Acc Chem Res* 12:276-281
2. Schwerdtfeger P, Seth M (2002). *Encyclopedia of Computational Chemistry: Relativistic effects of the superheavy elements.* Von Rague Schleyer P. https://doi.org/10.1002/0470845015.cra007
3. IUPAC Standards Online. *https://doi.org/10.1515/iupac* Accessed 17 April, 2024.
4. Schädel M, Brüchle W, Dressler R, et al. (1997). Chemical properties of element 106 (seaborgium). *Nature* 388:55–57
5. Guillaumont R, Adloff JP, Peneloux A (1989). Kinetic and thermodynamic aspects of tracer-scale and single atom chemistry. *Radiochim Acta* 46:169-176
6. Schädel M (2015). Chemistry of the superheavy elements. *Phil Trans R Soc A* 373:20140191
7. Oganessian YT, et al. (1999). Synthesis of superheavy nuclei in the 48-Ca + 244-Pu reaction. *Phys Rev Lett* 83:3154-3157
8. Oganessian YT, et al. (1999). Synthesis of nuclei of the superheavy element 114 in reactions induced by 48Ca. *Nature* 400:242–245
9. Oganessian YT, et al. (2000). Synthesis of superheavy nuclei in the 44-Ca + 244-Pu reaction: 288-114. *Phys Rev C* 62:041604
10. Oganessian YT, et al. (2004). Measurements of cross sections for the fusion-evaporation reactions 244-Pu(48-Ca,xn)292-x-114 and 245-Cm(48-Ca,xn)293-x-116. *Phys Rev C* 69:054607
11. Stavsetra L, Gregorich KE, Dvorak J, Ellison PA, Dragojevic I, Garcia MA, Nitsche H (2009). Independent verification of element 114 production in the 48-Ca + 242-Pu reaction. *Phys Rev Lett* 103:132502
12. Ellison PA, et al. (2010). New superheavy element isotopes: 242-Pu(48-Ca,5n)285-114. *Phys Rev Lett* 105:182701
13. Utyonkov VK, et al. (2015). Experiments on the synthesis of superheavy nuclei 284-Fl and 285-Fl in the 239,240-Pu + 48-Ca reactions. *Phys Rev C* 92:034609
14. Türler A, Gregorich KE (2014). *The Chemistry of Superheavy Elements: Experimental techniques*. Schädel M, Shaughnessy D. https://doi.org/10.1007/978-3-642-37466-1
15. Türler A, Pershina V (2013). Advances in the production and chemistry of the heaviest elements. *Chem Rev* 113:1237-1312
16. Schwarz WHE, van Wezenbeck E, Snijders JG, Baerends EJ (1989). The origin of relativistic effects of atomic orbitals. *J Phys B* 22:1515–1530
17. Baerends EJ, Schwarz WHE, Schwerdtfeger P, Snijders JG (1990). Relativistic atomic orbital contractions and expansions: magnitude and explanations. *J Phys B* 23:3225–3240
18. Fricke B (1975). Superheavy elements a prediction of their chemical and physical properties. *Struct Bond Berl Ger* 21:89-144
19. Pershina VG (1996). Electronic structure and the properties of the transactinides and their compounds. *Chem Rev* 96:1977-2010

20. Mewes JM, Smits OR, Kresse G, Schwerdtfeger P (2019). Copernicium: a relativistic noble liquid. *Angew Chem Int* 58:17964-17968
21. NUBASE2020, IAEA Nuclear Data Section. https://www-nds.iaea.org/relnsd/nubase/nubase_min.html Accessed 18 April, 2024.
22. Oganessian YT, et al. (2022). Investigation of 48-Ca-induced reactions with 242-Pu and 238-U targets at the JINR superheavy element factory. *Phys Rev C* 106:024612
23. Utyonkov VK, et al. (2018). Neutron-deficient superheavy nuclei obtained in the 240-Pu + 48-Ca reaction. *Phys Rev C* 97:014320
24. Yakushev A, Eichler R (2016). Gas-phase chemistry of element 114, flerovium. *EPJ Web Conf* 131:07003
25. Pitzer KS (1975). Are elements 112, 114, and 118 relatively inert gases? *J Chem Phys* 63:1032-1033
26. Hermann A, Furthmüller J, Gäggeler HW, Schwerdtfeger P (2010). Spin-orbit effects in structural and electronic properties for the solid state of the group-14 elements from carbon to superheavy element 114. *Phys Rev B* 82:155116
27. Ahmed MHH, Zaoui A, Ferhat M, Ahuja R (2017). Revisiting the ground state phase stability of super-heavy element flerovium. *Cogent Physics* 4:1380454
28. Florez E, Smits OR, Mewes JM, Jerabek P, Schwerdtfeger P (2022). From the gas phase to the solid state: the chemical bonding in the superheavy element flerovium. *J Chem Phys* 157:064304
29. Pershina V (2011). Relativistic electronic structure studies on the heaviest elements. *Radiochim Acta* 99:459-476
30. Eichler R, et al. (2010). Indication for a volatile element 114. *Radiochim Acta* 98:133-139
31. Yakushev A, et al. (2014). Superheavy element flerovium (element 114) is a volatile metal. *Inorg Chem* 53:1624-1629
32. Yakushev A, et al. (2022). On the adsorption and reactivity of element 114, flerovium. *Front Chem* 10:976635 https://www.frontiersin.org/journals/chemistry/articles/10.3389/fchem.2022.976635/full#h6 AVAILABLE UNDER PUBLIC LICENSE
33. Horwitz EP, McAlister DR, Dietz M (2006). Extraction chromatography versus solvent extraction: how similar are they? *Separation Science and Technology* 41(10):2163–2182
34. *Technical documents*. Triskem International. https://www.triskem-international.com/technical-documents.php Accessed 3 October, 2024.
35. Katykhin GS (1975). *Extraction Chromatography: Inert supports in column extraction chromatography*. Braun T, Ghersini G. https://doi.org/10.1016/S0301-4770(08)60971-9
36. Dietz ML, Horwitz EP (2000). Applications of extraction chromatography in the development of radionuclide generator systems for nuclear medicine. *Ind Eng Chem Res* 39(9):3181-3188
37. Markl P, Schmid ER (1975*). Extraction Chromatography: Techniques in column extraction chromatography.* Braun T, Ghersini G. https://doi.org/10.1016/S0301-4770(08)60969-0
38. Kovalenko O, Baulin V, Baulin D, Tsivadze A (2021). Solvent-impregnated resins based on the mixture of (2-diphenylphosphoryl)-4-ethylphenoxy)methyl)diphenylphosphine oxide and ionic liquid for Nd(II) recovery from nitric acid media. *Molecules* 26:2440
39. Rydberg J, Cox M, Musikas C, Choppin GR (2004). *Solvent Extraction Principles and Practice*, 2nd ed. New York, NY: Marcel Dekker, Inc.

40. Kislik VS (2012). *Solvent Extraction: Classical and Novel Approaches*. Oxford, UK:Elsevier
41. Guseva LI, Tikhomirova GS (2002). A 211-Pb generator as a methodical approach to studying the chemistry of element 114 in solutions. *Radiochem* 44(2):167-170
42. Guseva LI (2007). A study of the ion-exchange behavior of Pb in dilute HBr solutions. *Radiochem* 49:84-88
43. Despotopulos JD, Kmak KN, Moody KJ, Shaughnessy DA (2018). Development of a 212Pb and 212Bi generator for homolog studies of flerovium and moscovium. *J Radioanal Nucl Chem* 317: 473-477
44. Despotopulos JD, Kmak KN, Gharibyan N et al. (2018). Studies of the homologs and pseudo-homologs of flerovium with crown ether based extraction chromatography resins. *J Radioanal Nucl Chem* 318:1821-1926
45. Despotopulos JD, Kmak KN, Valdez CA, Moody KJ, Shaughnessy DA (2018). *Studies of flerovium homologs with thiacrown ethers*. LLNL-PRES-747949
46. Despotopulos JD (2015). *Studies of flerovium and element 115 homologs with macrocyclic extractants.* [Doctoral Dissertation, University of Nevada, Las Vegas]
47. Baumann TF, Reynolds JG, Fox GA (2000). Polymer pendant crown thioethers: synthesis, characterization and Hg(II) extraction studies of polymer-supported thiacrowns ([14]aneS4 and [17]aneS5). *React Funct Polym* 44(2):111-120
48. Baumann TF, Reynolds JG, Fox GA (1998). Polymer pendant crown thioethers: synthesis and Hg(II) extraction studies of a novel thiacrown polymer. *Chem Commun* 16:1637-1638
49. DeSimone RE, Glick MD (1976). Structures of the macrocyclic polythiaether 1,4,8,11-tetrathiacyclotetradecane and implications for transition-metal chemistry. *J Am Chem Soc* 98(3):762-767
50. Robilotto TJ (2011). *Synthesis and characterization of (phosphine)- and (N-heterocyclic carbene)gold(I) halides, azides, alkynyls, triazoles, and dendrimers and the synthesis and characterization of gold(I) thiacrown macrocycles*. [Doctoral Dissertation, Case Western Reserve University]
51. Konczyk J, Nowik-Zajac A, Kozlowski C (2016). Calixarene-based extractants for heavy metal ions removal from aqueous solutions. *Sep Sci Tech* 51(14):2394-2410
52. Khopkar SM (2008). *Analytical Chemistry of Macrocyclic and Supramolecular Compounds*, 2nd ed. New Delhi: Narosa Publishing House Pvt. Ltd.
53. Smith GF, Margerum DW (1975). Diminution of the macrocyclic effect for nickel(II) complexes of thioethers in nonaqueous solvents. *J Chem Soc Chem Commun* 19:807-808
54. Izatt RM, Haymore BL, Christensen J (1972). A stable OH3+–cyclic polyether complex characterised by infrared spectroscopy. *J Chem Soc Chem Comm* 23:1308-1309
55. Sudowe R, Calvert MG, Düllmann CE, Farina LM, Folden CM, Gregorich KE, Gallaher SEH, Hoffman DC, Nelson SL, Phillips, DC, Schwantes JM, Wilson RE, Zielinski, PM, Nitsche H (2006). Extraction of short-lived zirconium and hafnium isotopes using crown ethers: A model system for the study of rutherfordium. *Radiochim Acta* 94(3)123-129
56. Gutsche CD (1983). Calixarenes. *ACS Acc Chem Res* 16:161-170
57. Gutsche CD (2008). *Calixarenes: An Introduction*, 2nd Ed. Royal Society of Chemistry https://doi.org/10.1039/9781847558190

58. Boston A, Lee EK, Crawford J, Hanes R, Bartsch R (2012). New di-ionizable p-tert-butylcalix[4]arene-1,2-crown-4 ligands: synthesis and divalent metal ion extraction. *Tetrahedron* 68:10241-10251
59. NUBASE2020, IAEA Nuclear Data Section. https://www-nds.iaea.org/relnsd/nubase/nubase_min.html Accessed 18 April, 2024.
60. Horwitz EP, Dietz ML, Rhoads S, Felinto C, Gale NH, Houghton J (1994). A lead-selective chromatographic resin and its application to the isolation of lead from geological samples. *Anal Chim Acta* 292:263-273
61. Pb Resin, Eichrom Technologies. https://www.eichrom.com/products/pb-resin/ Accessed 3 October, 2024.
62. L'Annunziata MF (2003). *Handbook of Radioactivity Analysis*, 2nd Ed. San Diego: Academic Press, Elsevier
63. Knoll GF (2010). *Radiation Detection and Measurement*. Hoboken: John Wiley & Sons
64. Iki N, Kabuto C, Fukushima T, Kumagai H, Takeya H, Miyanari S, Miyashi T, Miyano S (2000). Synthesis of p-tert-butylthiacalix[4]arene and its inclusion property. *Tetrahedron* 56(11):1437-1443
65. Zhou H, Suroweic K, Purkiss DW, Bartsch RA (2005). Proton di-ionizable p-tert-butylcalix[4]arene-crown-6 compounds in cone, partial-cone and 1,3 alternate conformations: synthesis and alkaline earth metal cation extraction. *Org Biomol Chem* 3:1676-1684

APPENDIX I: MATERIALS AND REAGENTS

Hydrochloric Acid, ULTREX II Ultrapure

CAS: 7647-01-0

Nitric Acid, ULTREX II Ultrapure

CAS: 7697-37-2

Carbon Tetrachloride, Reagent Grade

CAS: 56-23-5

Chloroform, ACS Reagent

CAS: 67-66-3

4-tert-Butylcalix[4]arene

CAS: 60705-62-6

4-tert-Butylsulfonylcalix[4]arene

CAS: 204190-49-8

4-tert-Butylthiacalix[4]arene

CAS: 182496-55-5

4-Sulfocalix[4]arene

CAS: 112269-92-8

4′,4″(5″)-Di-tert-butyldicyclohexano-18-crown-6, ≥90% (GC)

CAS: 223719-29-7

Pb Resin (50-100 µm), Eichrom Technologies

Part No: PB-B50-S

Table 5. Physical and chemical properties of Pb resin from the manufacturer[34]

Density: 0.37 g/mL
Capacity: 29 mg Pb/g resin
Conversion Factor, D_w/k': 1.82

Eppendorf ThermoMixer C

Whatman 0.45 µm polytetrafluoroethylene filter

EXELINT 3 mL polypropylene Luer-lock syringe

RAININ 100 µL Pipet-Lite LTS pipette

RAININ 1000 µL Pipet-Lite LTS pipette

Thermo Scientific 1.5 mL microcentrifuge tubes

^{212}Pb 1µCi mL^{-1} in 2 mol L^{-1} HCl

APPENDIX II: RAW DATA

Table 6. Raw data for Figure 17, 21 & 33

HCl Concentration (M)	k'_{Pb}	HNO_3 Concentration (M)	k'_{Pb}
0.1	136.00 ± 14.15	0.5	721.43 ± 46.21
0.4	158.45 ± 10.52	1	822.40 ± 71.74
0.8	150.29 ± 10.05	2	750.67 ± 56.44
1	136.33 ± 8.90	4	558.91 ±27.38
1.5	100.56 ± 6.32	6	379.15 ±12.87
2	71.60 ± 4.43	8	186.53 ± 8.27
		10	118.23 ± 5.21

Table 7. Raw data for Figure 18 & 33

HNO_3 Concentration (M)	D_w	k'
0.5	1433.29 ± 282.51	787.52 ± 129.44
1	2257.71 ± 232.09	1240.50 ± 127.52
2	1901.38 ± 239.17	1044.71 ± 131.41
4	1030.37 ± 45.02	566.14 ± 24.74
6	527.31 ± 20.77	289.73 ± 11.41
8	352.48 ± 32.21	193.67 ± 17.70
10	216.26 ± 23.60	118.82 ± 12.97

Table 8. Raw data for Figures 19 & 20

HCl Concentration (M)	Batch 1 k'	Batch 2 k'
0.1	1088.05 ± 267.98	1104.61 ± 47.64
0.4	1373.93 ± 139.83	1460.22 ± 70.14
0.8	1045.96 ± 116.46	1135.48 ± 49.40
1	1036.41 ± 77.36	1039.03 ± 43.34
0.5	659.08 ± 42.06	664.80 ± 24.10
2	369.56 ± 44.15	383.35 ± 11.79

Table 9. Raw data for Figure 21

HCl Concentration (M)	$k'_{average}$
0.1	1096.33 ± 8.28
0.4	1417.07 ± 43.14
0.8	1090.68 ± 44.72
1	1037.71 ± 1.31
0.5	661.94 ± 2.86
2	376.46 ± 6.90

Table 10. Raw data for Figure 22

Time (s)	D_w
30	97.48 ± 4.21
68	201.12 ± 6.94
301	393.57 ± 11.30
898	448.79 ± 12.51
1798	466.69 ± 12.88
3599	494.52 ± 13.64
10799	531.46 ± 14.34
21598	529.04 ± 14.32
32397	530.97 ± 14.04

Table 11. Raw data for Figure 23

HCl Concentration (M)	D
0.04	0.315 ± 0.055
0.06	0.198 ± 0.045
0.08	0.153 ± 0.041
0.1	0.180 ± 0.044
0.2	0.156 ± 0.042
0.4	0.212 ± 0.046
0.8	0.097 ± 0.038
1	0.028 ± 0.010

Table 12. Raw data for Figure 24

HCl Concentration (M)	D
0.04	0.261 ± 0.053
0.06	0.309 ± 0.057
0.08	0.205 ± 0.047
0.1	0.291 ± 0.055
0.2	0.166 ± 0.044
0.4	0.215 ± 0.048
0.8	0.162 ± 0.044
1	0.167 ± 0.045

Table 13. Raw data for Figures 25 & 28

HCl Concentration (M)	D
0.01	0.544 ± 0.133
0.02	0.315 ± 0.033
0.03	0.374 ± 0.180
0.04	0.248 ± 0.115
0.06	0.164 ± 0.027
0.08	0.173 ± 0.076
0.1	0.183 ± 0.078
0.2	0.279 ± 0.092
0.4	0.159 ± 0.063
0.8	0.223 ± 0.101
1	0.120 ± 0.026

Table 14. Raw data for Figures 26 & 28

HCl Concentration (M)	D
0.01	0.829 ± 0.299
0.02	0.618 ± 0.228
0.03	0.394 ± 0.132
0.04	0.685 ± 0.133
0.06	0.483 ± 0.055
0.08	0.281 ± 0.124
0.1	0.355 ± 0.097
0.2	0.316 ± 0.052
0.4	0.297 ± 0.059
0.8	0.197 ± 0.071
1	0.167 ± 0.076

Table 15. Raw data for Figures 27 & 28

HCl Concentration (M)	D		
0.01	1.986	±	0.435
0.02	0.705	±	0.253
0.03	0.392	±	0.026
0.04	0.588	±	0.107
0.06	0.448	±	0.088
0.08	0.383	±	0.107
0.1	0.366	±	0.028
0.2	0.320	±	0.095
0.4	0.344	±	0.071
0.8	0.222	±	0.039
1	0.299	±	0.099

Table 16. Raw data for Figure 29

HCl Concentration (M)	D		
0.08	0.267	±	0.091
0.1	0.269	±	0.025
0.2	0.242	±	0.021
0.4	0.346	±	0.077
0.8	0.261	±	0.090
1	0.242	±	0.162
1.5	0.195	±	0.072
2	-		-

Table 17. Raw data for Figure 30

[DtBuCH18C6]	log [DtBuC18C6]	D	log D
0.001	-3	0.054	-1.268
0.005	-2.301	0.251	-0.600
0.01	-2	0.519	-0.285
0.05	-1.301	3.23	0.509
0.1	-1	6.01	0.779

Table 18. Raw data for Figure 31

[HCl]	log [HCl]	D	log D
0.2	-0.699	0.165 ± 0.089	-0.783
0.4	-0.3979	0.278 ± 0.041	-0.556
0.8	-0.0969	0.426 ± 0.132	-0.371

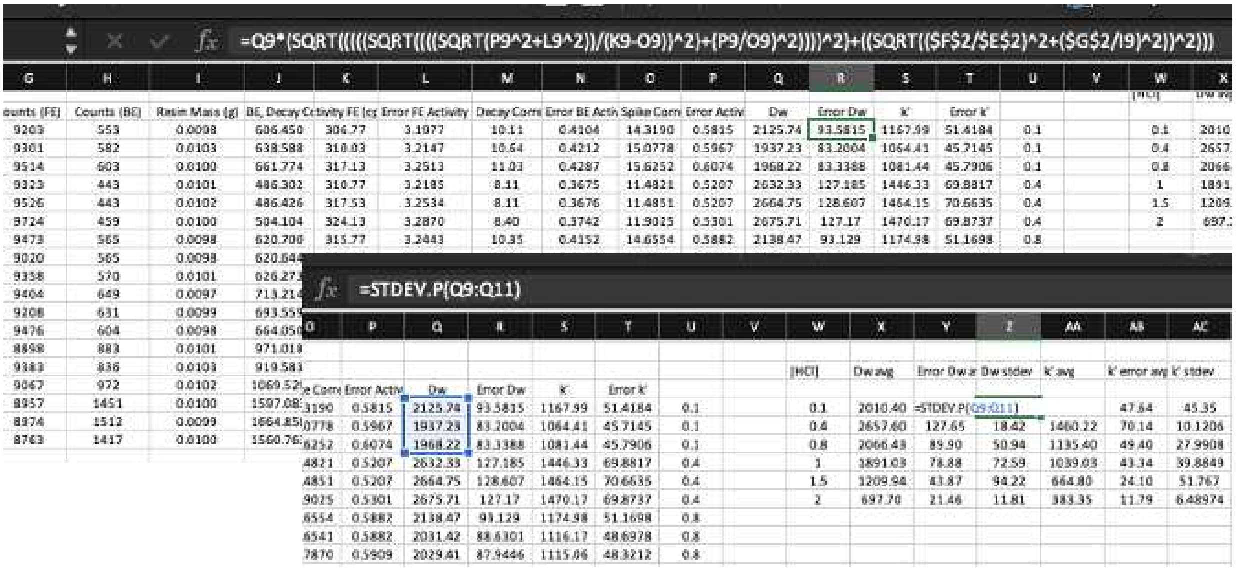

```
=Q9*(SQRT(((((SQRT((((SQRT(P9^2+L9^2))/(K9-O9))^2)+(P9/O9)^2))))^2)+((SQRT(($F$2/$E$2)^2+($G$2/I9)^2))^2)))
```

G	H	I	J	K	L	M	N	O	P	Q	R	S	T	U	V	W	X
ounts (FE)	Counts (BE)	Resin Mass (g)	BE, Decay C	ctivity FE (c	Error FE Activity	Decay Corr	Error BE Acti	Spike Corr	Error Activ	Dw	Error Dw	k'	Error k'			[HCl]	Dw av
9203	553	0.0098	606.450	306.77	3.1977	10.11	0.4104	14.3190	0.5815	2125.74	93.5815	1167.99	51.4184	0.1		0.1	2010
9301	582	0.0103	638.588	310.03	3.2147	10.64	0.4212	15.0778	0.5967	1937.23	83.2004	1064.41	45.7145	0.1		0.4	2657.
9514	603	0.0100	661.774	317.13	3.2513	11.03	0.4287	15.6252	0.6074	1968.22	83.3388	1081.44	45.7906	0.1		0.8	2066.
9323	443	0.0101	486.302	310.77	3.2185	8.11	0.3675	11.4821	0.5207	2632.33	127.185	1446.33	69.8817	0.4		1	1891.
9526	443	0.0102	486.426	317.53	3.2534	8.11	0.3676	11.4851	0.5207	2664.75	128.607	1464.15	70.6635	0.4		1.5	1209.
9724	459	0.0100	504.104	324.13	3.2870	8.40	0.3742	11.9025	0.5301	2675.71	127.17	1470.17	69.8737	0.4		2	697.
9473	565	0.0098	620.700	315.77	3.2443	10.35	0.4152	14.6554	0.5882	2138.47	93.129	1174.98	51.1698	0.8			
9020	565	0.0098	620.644														
9358	570	0.0101	626.273														
9404	649	0.0097	713.214														
9208	631	0.0099	693.559														
9476	604	0.0098	664.050														
8898	883	0.0101	971.018														
9383	836	0.0103	919.583														
9067	972	0.0102	1069.52														
8957	1451	0.0100	1597.08														
8974	1512	0.0099	1664.85														
8763	1417	0.0100	1560.76														

```
=STDEV.P(Q9:Q11)
```

O	P	Q	R	S	T	U	V	W	X	Y	Z	AA	AB	AC
e Corr	Error Activ	Dw	Error Dw	k'	Error k'			[HCl]	Dw avg	Error Dw a	Dw stdev	k' avg	k' error avg	k' stdev
3190	0.5815	2125.74	93.5815	1167.99	51.4184	0.1		0.1	2010.40	=STDEV.P(Q9:Q11)			47.64	45.35
0778	0.5967	1937.23	83.2004	1064.41	45.7145	0.1		0.4	2657.60	127.65	18.42	1460.22	70.14	10.1206
6252	0.6074	1968.22	83.3388	1081.44	45.7906	0.1		0.8	2066.43	89.90	50.94	1135.40	49.40	27.9908
4821	0.5207	2632.33	127.185	1446.33	69.8817	0.4		1	1891.03	78.88	72.59	1039.03	43.34	39.8849
4851	0.5207	2664.75	128.607	1464.15	70.6635	0.4		1.5	1209.94	43.87	94.22	664.80	24.10	51.767
9025	0.5301	2675.71	127.17	1470.17	69.8737	0.4		2	697.70	21.46	11.81	383.35	11.79	6.48974
6554	0.5882	2138.47	93.129	1174.98	51.1698	0.8								
6541	0.5882	2031.42	88.6301	1116.17	48.6978	0.8								
7870	0.5909	2029.41	87.9446	1115.06	48.3212	0.8								

Figure 34. Propagation of uncertainty from counting statistics

APPENDIX III: PERMISSIONS

Some of the figures used in this thesis were reused from a variety of documents. Those available in the public domain and those obtained from government documents were cited accordingly. Figures which require permission for reuse are identified along with the applicable permission-granting documents in this appendix.

Figure 2:

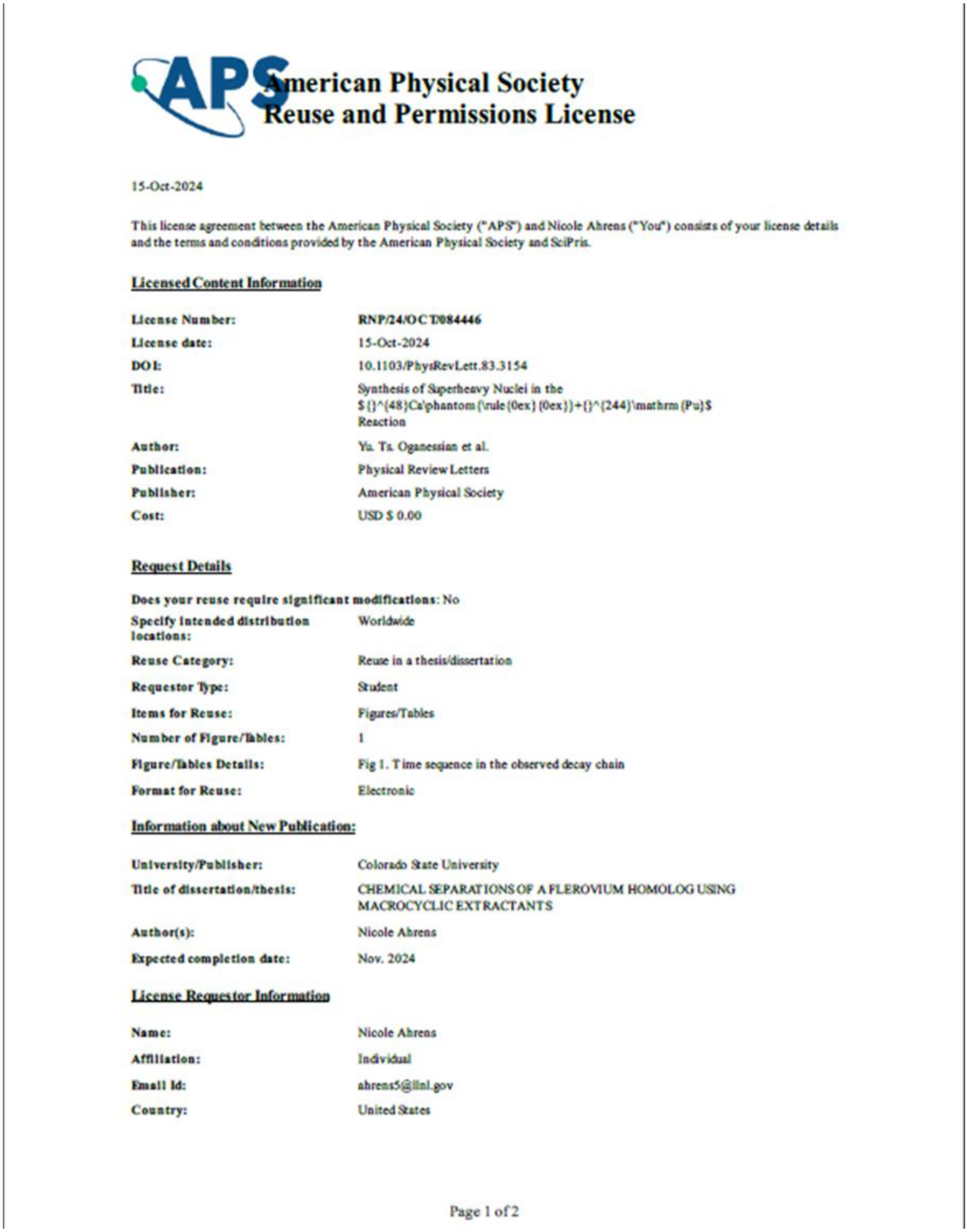

American Physical Society
Reuse and Permissions License

15-Oct-2024

This license agreement between the American Physical Society ("APS") and Nicole Ahrens ("You") consists of your license details and the terms and conditions provided by the American Physical Society and SciPris.

Licensed Content Information

License Number:	**RNP/24/OCT/084446**
License date:	15-Oct-2024
DOI:	10.1103/PhysRevLett.83.3154
Title:	Synthesis of Superheavy Nuclei in the `${}^{48}Ca\phantom{\rule{0ex}{0ex}}+{}^{244}\mathrm{Pu}$` Reaction
Author:	Yu. Ts. Oganessian et al.
Publication:	Physical Review Letters
Publisher:	American Physical Society
Cost:	USD $ 0.00

Request Details

Does your reuse require significant modifications: No

Specify intended distribution locations:	Worldwide
Reuse Category:	Reuse in a thesis/dissertation
Requestor Type:	Student
Items for Reuse:	Figures/Tables
Number of Figure/Tables:	1
Figure/Tables Details:	Fig 1. Time sequence in the observed decay chain
Format for Reuse:	Electronic

Information about New Publication:

University/Publisher:	Colorado State University
Title of dissertation/thesis:	CHEMICAL SEPARATIONS OF A FLEROVIUM HOMOLOG USING MACROCYCLIC EXTRACTANTS
Author(s):	Nicole Ahrens
Expected completion date:	Nov. 2024

License Requestor Information

Name:	Nicole Ahrens
Affiliation:	Individual
Email Id:	ahrens5@llnl.gov
Country:	United States

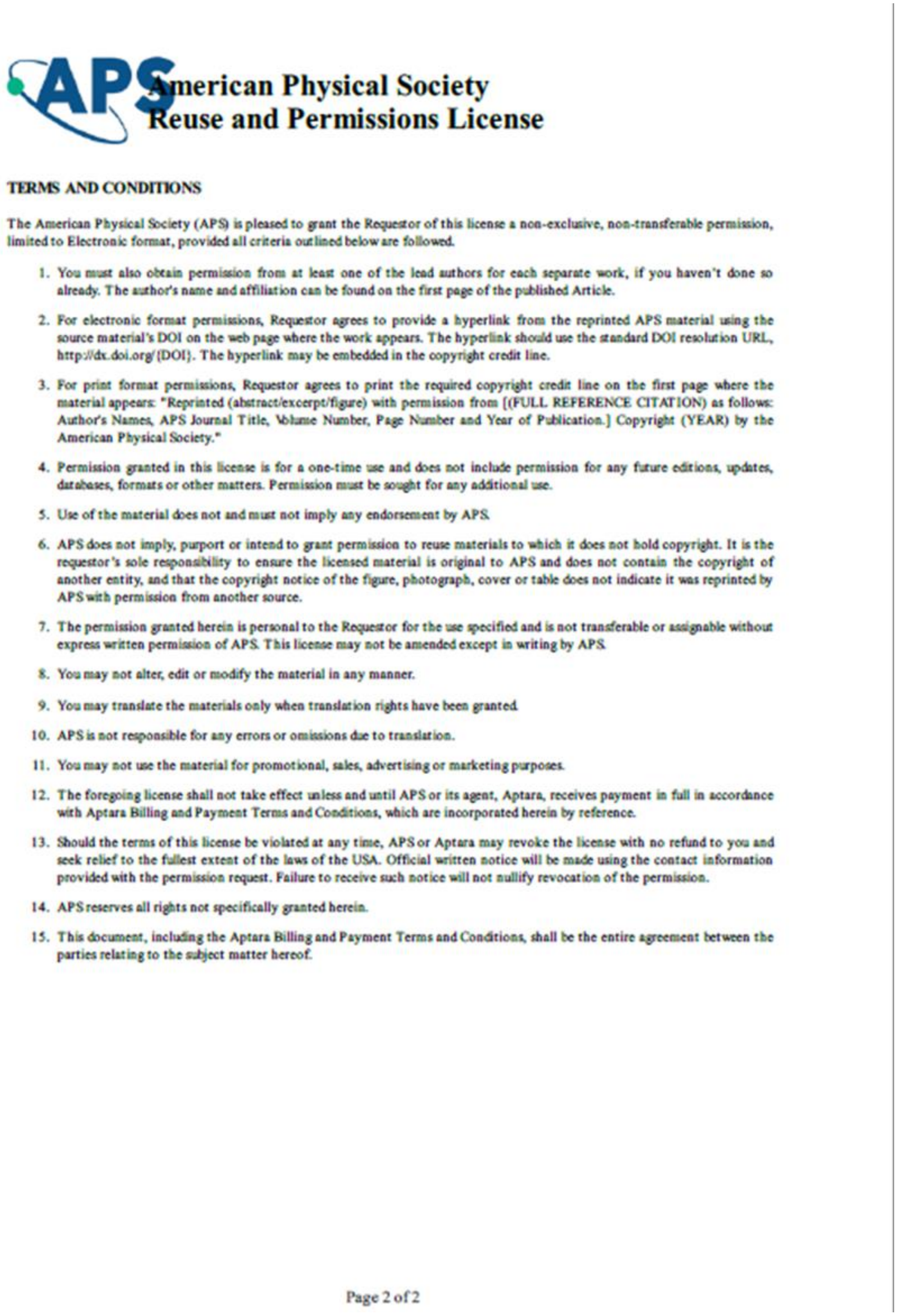

American Physical Society
Reuse and Permissions License

TERMS AND CONDITIONS

The American Physical Society (APS) is pleased to grant the Requestor of this license a non-exclusive, non-transferable permission, limited to Electronic format, provided all criteria outlined below are followed.

1. You must also obtain permission from at least one of the lead authors for each separate work, if you haven't done so already. The author's name and affiliation can be found on the first page of the published Article.
2. For electronic format permissions, Requestor agrees to provide a hyperlink from the reprinted APS material using the source material's DOI on the web page where the work appears. The hyperlink should use the standard DOI resolution URL, http://dx.doi.org/{DOI}. The hyperlink may be embedded in the copyright credit line.
3. For print format permissions, Requestor agrees to print the required copyright credit line on the first page where the material appears: "Reprinted (abstract/excerpt/figure) with permission from [(FULL REFERENCE CITATION) as follows: Author's Names, APS Journal Title, Volume Number, Page Number and Year of Publication.] Copyright (YEAR) by the American Physical Society."
4. Permission granted in this license is for a one-time use and does not include permission for any future editions, updates, databases, formats or other matters. Permission must be sought for any additional use.
5. Use of the material does not and must not imply any endorsement by APS.
6. APS does not imply, purport or intend to grant permission to reuse materials to which it does not hold copyright. It is the requestor's sole responsibility to ensure the licensed material is original to APS and does not contain the copyright of another entity, and that the copyright notice of the figure, photograph, cover or table does not indicate it was reprinted by APS with permission from another source.
7. The permission granted herein is personal to the Requestor for the use specified and is not transferable or assignable without express written permission of APS. This license may not be amended except in writing by APS.
8. You may not alter, edit or modify the material in any manner.
9. You may translate the materials only when translation rights have been granted.
10. APS is not responsible for any errors or omissions due to translation.
11. You may not use the material for promotional, sales, advertising or marketing purposes.
12. The foregoing license shall not take effect unless and until APS or its agent, Aptara, receives payment in full in accordance with Aptara Billing and Payment Terms and Conditions, which are incorporated herein by reference.
13. Should the terms of this license be violated at any time, APS or Aptara may revoke the license with no refund to you and seek relief to the fullest extent of the laws of the USA. Official written notice will be made using the contact information provided with the permission request. Failure to receive such notice will not nullify revocation of the permission.
14. APS reserves all rights not specifically granted herein.
15. This document, including the Aptara Billing and Payment Terms and Conditions, shall be the entire agreement between the parties relating to the subject matter hereof.

Page 2 of 2

Figure 3: https://creativecommons.org/licenses/by/4.0/#ref-appropriate-credit

Figure 12:

ELSEVIER LICENSE
TERMS AND CONDITIONS
Oct 15, 2024

This Agreement between Nicole Ahrens ("You") and Elsevier ("Elsevier") consists of your license details and the terms and conditions provided by Elsevier and Copyright Clearance Center.

License Number	5890341296045
License date	Oct 15, 2024
Licensed Content Publisher	Elsevier
Licensed Content Publication	Analytica Chimica Acta
Licensed Content Title	A lead-selective extraction chromatographic resin and its application to the isolation of lead from geological samples
Licensed Content Author	E. Philip Horwitz,Mark L. Dietz,Susan Rhoads,Claudia Felinto,Noel H. Gale,Judith Houghton
Licensed Content Date	Jul 11, 1994
Licensed Content Volume	292
Licensed Content Issue	3
Licensed Content Pages	11
Start Page	263
End Page	273
Type of Use	reuse in a thesis/dissertation
Portion	figures/tables/illustrations
Number of figures/tables/illustrations	1
Format	electronic
Are you the author of this Elsevier article?	No
Will you be translating?	No
Title of new work	CHEMICAL SEPARATIONS OF A FLEROVIUM HOMOLOG USING MACROCYCLIC EXTRACTANTS
Institution name	Colorado State University
Expected presentation date	Oct 2024
Portions	Fig 2. Nitric acid and hydrochloric acid dependencies of k' for Pb